SEISMIC ATTRIBUTES AND ADVANCED COMPUTER ALGORITHM TO PREDICT FORMATION PORE PRESSURE: QALIBAH FORMATION OF NORTHWEST SAUDI ARABIA

BY

ABDOULSHAKOUR M NOUR

A Thesis Presented to the

DEANSHIP OF GRADUATE STUDIES

KING FAHD UNIVERSITY OF PETROLEUM & MINERALS

DHAHRAN, SAUDI ARABIA

In Partial Fulfillment of the
Requirements for the Degree of

MASTER OF SCIENCE

In

GEOPHYSICS

APRIL 2013

KING FAHD UNIVERSITY OF PETROLEUM AND MINERSLS

DHAHRAN 31261, SAUDI ARABIA.

DEANSHIP OF GRADUATE STUDIES

This thesis, written by **Abdoulshakour M Nour** under the direction of his thesis advisor and approved by his thesis committee, has been presented to and accepted by the Dean of Graduate Studies, in partial fulfillment of the requirements for the degree of **MASTER OF SCIENCE IN GEOPHYSICS.**

Thesis Committee

Prof. Gabor Korvin
Thesis Advisor

Dr. Abdulaziz Al-Shaibani
Department Chairman

Dr. AbdulLatif Osman
Member

Dr. Salaam Zummo
Dean of Graduate Studies

Dr. Saleh Al-Dossary
Member

18/5/13

Date

DEDICATION

This work is dedicated to my lovely wife and four beautiful children who offered me unconditional love and support throughout my studies at KFUPM and completion of this thesis.

ACKNOWLEDGEMENTS

I owe an immense debt of gratitude to my adviser Dr. Professor Gabor Korvin for his continued guidance, patience, motivation, enthusiasm and extensive knowledge. His unwavering counsel and direction helped me greatly in completing my Master's degree program including this thesis. I would like to also extend sincere thanks to my thesis advisory committee member Dr. Osman M Abdullatif, for his excellent advice and careful guidance which were invaluable to my success in completing this thesis.

I am truly thankful, from the bottom of my heart, to my thesis advisory committee member and colleague Dr. Salah Al-Dossary for his ideas, analysis, and unwavering support throughout the process of researching and writing this thesis. A special thanks goes to my colleagues and member of management in Saudi Aramco Exploration Application Services Department, Khaled Al-Bassam, Abdullah Al-Eidi, Adel Al-Naji Abdulkarim Al-Zahrani, and Jinsong Kong, whose support was crucial to the completion of this thesis work.

Another group that deserves my sincere thanks is the Saudi Aramco Geophysical Technical Services Division team members and member of management, Dr. Mohammad Al-Otaibi, Aiman Bakhorji, and Husam Mustafa, for their advice, support, frank discussions, and hospitality during my two-month research assignment.

Finally, I would be remiss without mentioning Dr. Nasher BenHasan, whose extreme generosity with his time, and in-depth discussion of the subject matter was instrumental in formulating my own conclusions. To all, I extend my sincere gratitude.

TABLE OF CONTENTS

LIST OF TABLES

LIST OF FIGURES

THESIS ABSTRACT

Name: Abdoulshakour Mark Nour

Thesis Title: Seismic Attributes and Advanced Computer Algorithm to Predict Formation Pore Pressure: Qalibah Formation of Northwest Saudi Arabia

Major Field: Geophysics

Date: April, 2013

Oil and gas exploration professionals have long recognized the importance of predicting pore pressure before drilling wells. Pre-drill pore pressure estimation not only helps with drilling wells safely but also aids in the determination of formation fluids migration and seal integrity. With respect to the hydrocarbon reservoirs, the appropriate drilling mud weight is directly related to the estimated pore pressure in the formation. If the mud weight is lower than the formation pressure, a blowout may occur, and conversely, if it is higher than the formation pressure, the formation may suffer irreparable damage due to the invasion of drilling fluids into the formation. A simple definition of pore pressure is the pressure of the pore fluids in excess of the hydrostatic pressure.

In this thesis, I investigated the utility of advance computer algorithm called Support Vector Machine (SVM) to learn the pattern of high pore pressure regime, using seismic attributes such as Instantaneous phase, t*Attenuation, Cosine of Phase, Vp/Vs ratio, P-Impedance, Reflection Acoustic Impedance, Dominant frequency and one well attribute

(Mud-Weigh) as the learning dataset. I applied this technique to the over pressured Qalibah formation of Northwest Saudi Arabia.

The results of my research revealed that in the Qalibah formation of Northwest Saudi Arabia, the pore pressure trend can be predicted using SVM with seismic and well attributes as the learning dataset. I was able to show the pore pressure trend at any given point within the geographical extent of the 3D seismic data from which the seismic attributes were derived. In addition, my results surprisingly showed the subtle variation of pressure within the thick succession of shale units of the Qalibah formation.

Master of Science in Geophysics

King Fahd University of Petroleum and Minerals

Dhahran, Saudi Arabia

April, 2013

THESIS ABSTRACT IN ARABIC

الخلاصة

الأسم: عبد الشكور مارك نور

عنوان الرسالة: استخدام الخصائص الزلزالية ولوغريثم حاسوبي متقدم للتنبؤ بالضغ المسامي في مكون قليبه في شمال غرب المملكة العربية السعودية

التخصص: جيوفيزياء

التاريخ: ابريل 2013 م

يعتبر التنبؤ بالضغط المسامي في عمليات التنقيب عن البترول من الأشياء المهمة قبل حفر الآبار. التنبؤ بالضغط قبل الحفر يساعد على سلامة عملية الحفر وعلى معرفة حركة السوائل في التكوينات الصخرية وعلى متانة وتكامل صخور غطاء المكامن البترولية. في البترولية المكامن وجد أن وزن الطين المناسب للحفر يتناسب مباشرة مع الضغط المسامي في المكامن. إذا كان وزن طين الحفر أقل من الضغط المسامي في التكوينات الصخرية فإن هذا يؤدي إلى انفجار خارجي في البئر. أما إذا كان وزن طين الحفر أعلى فإن هذا يؤدي إلى دخول سوائل الحفر إلى داخل التكوينات الصخرية

مما يؤدي إلى التسبب في ضرر بالغ للمكمن. يعرف الضغط المسامي على إنه ضغط سوائل المسام الزائد من الضغط المائي.

في هذه الرسالة تم دراسة استخدام لوغريثم حاسوبي متقدم (SVM) بالإضافة إلى استخدام الخصائص الزلزالية للتعرف على نمط الضغط المسامي العالي. لقد تم تطبيق هذه الدراسة على مكون قليبه، ذات الضغط العالي، في شمال المملكة العربية السعودية.

كشفت نتائج الدراسة على مكون قليبه في شمال المملكة إلى أنه يمكن التنبؤ بنمط الضغط المسامي وذلك باستخدام الخصائص الزلزالية والبئر واللوغريثم الحاسوبي المتقدم. تمكنت الدراسة من تحديد الضغط المسامي في أي نقطة على الامتداد الجغرافي للمعلومات الزلزالية التي منها اخذت الخصائص الزلزالية التي استخدمت في هذه الدراسة. هذا بالإضافة فإن نتائج الدراسة أيضاً أشارت إلى التغيير في الضغط في التتابع الرسوبي لوحدات الشيل (Shale) في مكون قليبه.

درجةالماجستيرفي العاوم

جامعة الملك فهد للبترول والمعادن

الظهران - المملكة العربية السعودية

أبريل 2013م

CHAPTER 1

INTRODUCTION

1.0 Thesis Organization

In chapter one, I provide an introduction to the thesis topic, provide details about the mechanisms that result in over pressured formations, state the motivation behind this work, offer a review of previous work in the area of interest and state the methods that will be used to provide a reliable pore pressure prediction method based on seismic and well attributes. Chapter two describes the geological setting of the study area and main target formations. Chapter three reviews the seismic attributes that will be used to predict abnormally high formation pore-pressure. Chapter four will describe Support Vector Machine algorithm and how this technology can be utilized to find the best seismic attributes that can reliably predict abnormally high formation pore-pressure. Chapter five shows the application of the abnormally high pore-pressure prediction method to the Qalibah Formation in Northwest Saudi Arabia. Chapter six will provide final conclusions and recommendations.

1.1 Overview

Oil and gas exploration professionals have long recognized the importance of predicting pore-pressure before drilling wells. Pre-drill pore pressure estimation not only helps with drilling wells safely, but also aids in the determination of formation fluid migration and seal integrity. With respect to the hydrocarbon reservoirs, the appropriate drilling mud weight is directly related to the estimated pore pressure in the formation. If the mud weight is lower than the formation pressure, a blowout may occur and conversely, if it is higher than the formation pressure, the formation may suffer irreparable damage due to the invasion of drilling fluids. Experts estimate the cost of drilling wells in over-pressured formations to be over $20 million per well or $1.08 billion annually throughout the world (Dutta *et al.*, 2002).

Many of the world's prolific hydrocarbon bearing rocks are associated with the onset of higher formation pressures. A good example is the over pressured Tertiary sediments of South Louisiana, USA, from which more than half of the gas production is attributed to a 600 meter section around the onset of abnormally high pressure profile (Leach, 1994). The lower Qalibah Formation shale member in Northwest Saudi Arabia is considered both a source and reservoir rock that has high total organic content (TOC). Overpressure in the Qalibah Formation has been observed where formation hydrocarbons are unable to escape due to the sealing properties of the bounding formations (Faqira, 2010).

Formation over pressure is due to many factors that are related to the geologic, physical, geochemical and mechanical processes that the formation undergoes through time (Fertl, 1976). A simple definition of *pore pressure* is when the pore fluid pressure is greater than the hydrostatic pressure. Therefore a formation is under normal pressure when the fluids in the pore space are subject to hydrostatic pressure. This is the pressure required to lift

(raise) a column of fluids from the formation to a location on the surface. When the formation pressure is higher than the hydrostatic pressure, then the formation pressure is said to be abnormally high. The formation pressure could also be below the hydrostatic pressure, resulting in abnormally low formation pressure, although this situation is much rarer than the high pressured situation.

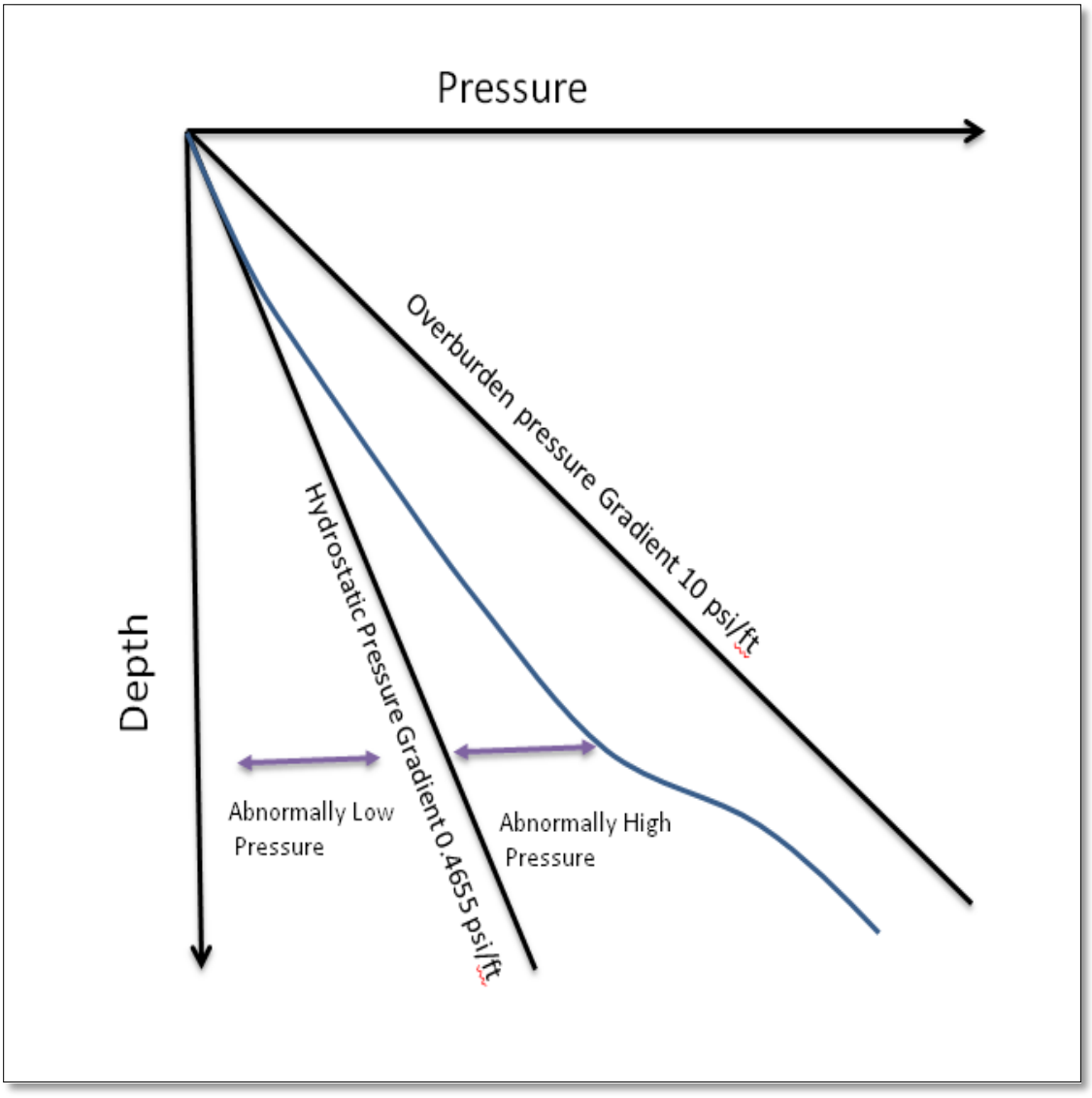

Figure 1: Formation Pressure Regimes

In normally pressured formations, the fluids in the pore space of the rock are only bearing the burden (weight) resulting from of the fluids above. The rock matrix and the interlocking grains of rock, support the weight of the overlying strata. The pore fluids have been drained from the pore spaces as the sediments were undergoing normal compaction and burial or due to other geological processes that allowed the formation fluids to escape. For sediments that are under abnormally high pressure, the fluids (liquids, gas, oil) locked in the pore cavities of the formation (between grains of rock) are bearing some of the weight of the overlying strata. The formation fluids have not had the chance to escape the pore space due to quick burial or other geological factors that impeded the movement of pore fluids such as impermeable formations sealing the rocks.

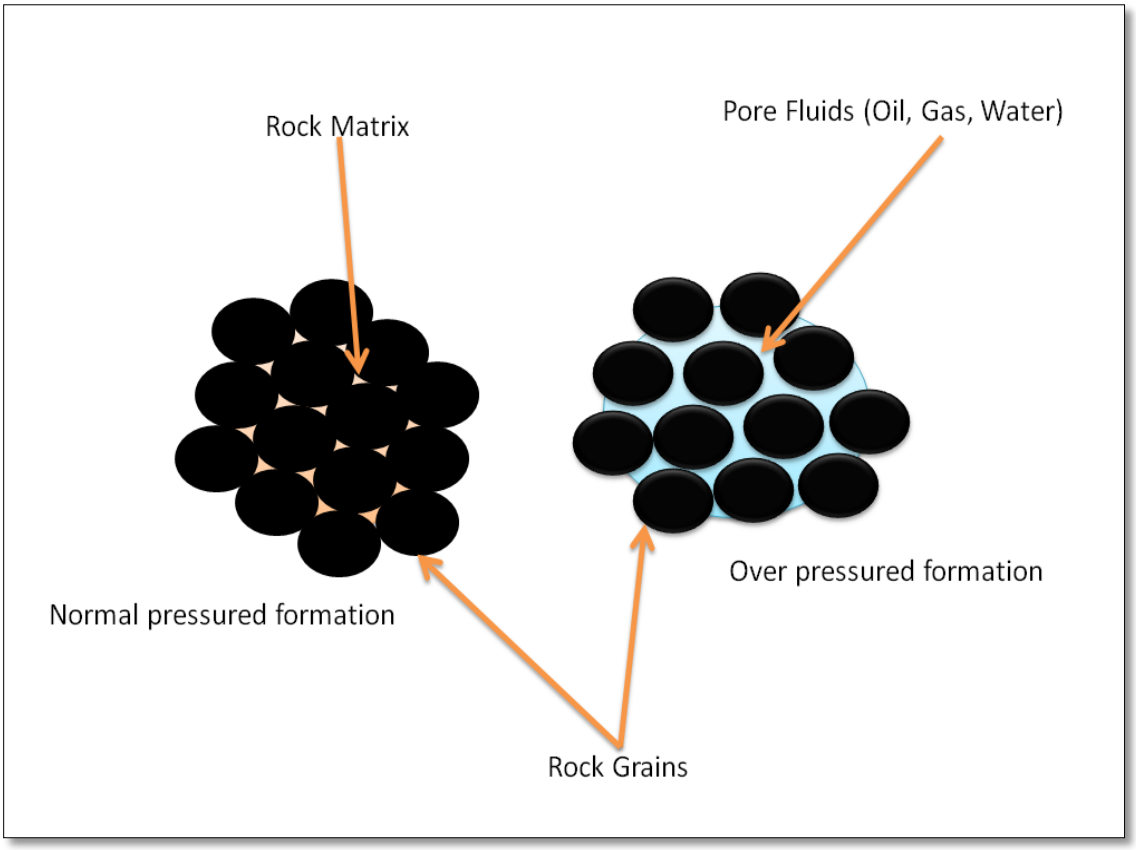

Figure 2: Normal and Abnormally high Formation Pressure

1.2 Causes of overpressure

Abnormally high formation pore pressure is caused by a number of geological processes that have influenced a given formation. The one factor that is common throughout is that the formation fluids in the pore space are trapped and thus carrying some of the load of the overlying strata. Major causes of high pore pressure that are discussed in the literature include compaction disequilibrium, diagenetic processes, aqua-thermal pressuring and hydrocarbon maturation (Mukerji, 2002).

Disequilibrium compaction results from inability of sediments to expel the content of their pore fluids as they undergo burial and sediment loading. One type of compaction disequilibria is the under-consolidated state of sediments after burial. In clayey sediments, clay particles have two oppositely charged surfaces. One surface is the edge of the clay particle which is positively charged while the other is the face of the particle which is negatively charged. Due to the electrostatic forces, clay particles tend to amass edge to face during compaction (See Figure 3).

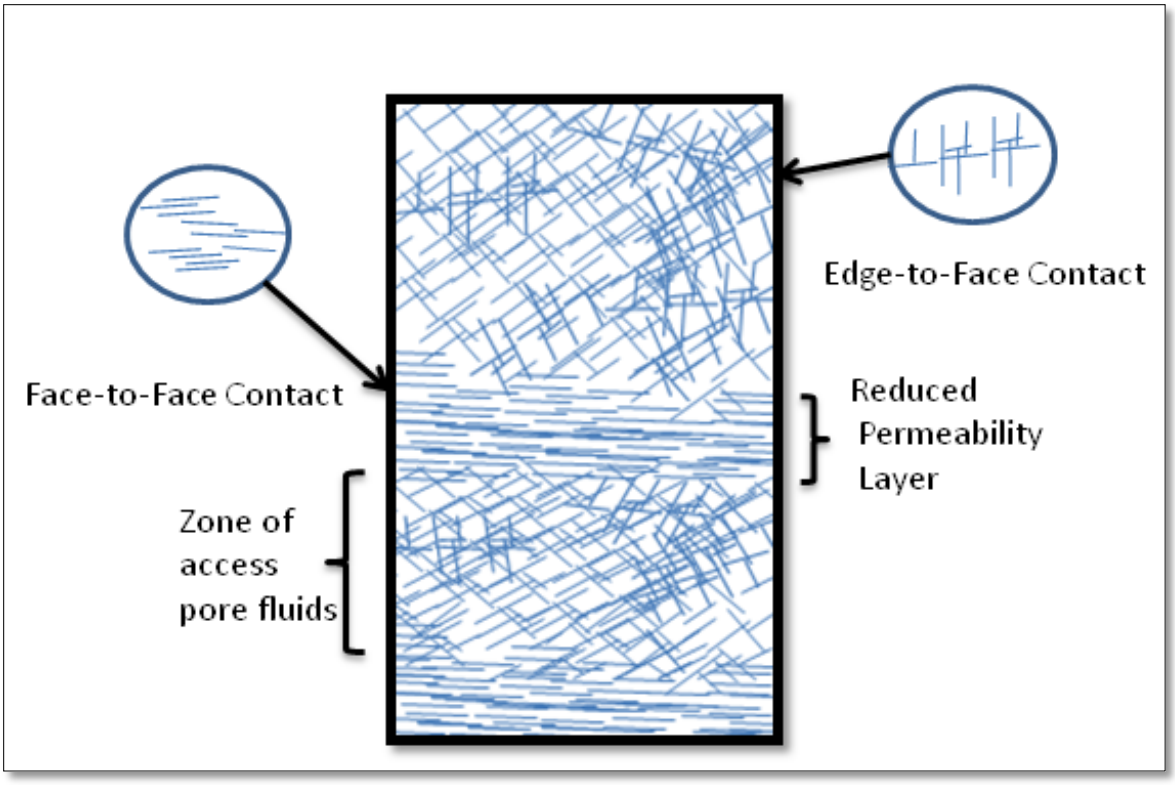

Figure 3: Schematic showing compaction of clay sediments during deposition (Modified after Schwehr, 2006)

During sediment loading, volume reduction causes the collapse of the clay structure and forms compacted face to face structures. High pressure is likely to result in areas were the rate of pore fluid escape cannot match the rate of sedimentation. The presence of layers that act as barriers to fluid upward movement will also contribute to trapping of the pore fluids in place, thus developing layers of excess fluid content. These layers would also reduce the normal clay compaction and prevent the edge-to-face alignment of the clay particles from changing it to face-to-face contacts (Schwehr, 2006).

Another major cause of high pore pressure is the physical or chemical alteration of sediments resulting from the higher temperature and pressure they are subjected to after burial. These altering processes are collectively known as diagenesis and could result in the generation of new minerals or recrystallization and lithification of existing minerals. These processes may

also lead to volume changes and water generation in the pore spaces of rocks, resulting in abnormally high pore pressure (Fertl, 1976).

A good example of this type of abnormally high formation pressure generation is the diagenetic conversion of clay minerals from Smectite to Illite. Upon burial, marine shale sediment clays are dominantly composed of Smectite of which Montmorillonite is the most common form. Montmorillonite is characterized by a swelling lattice and contains significant volume of water during initial deposition. Montmorillonite is naturally alkaline and contains significant amounts of ions of calcium and magnesium but contain very little ions of potassium. The water is contained in both the interlayer space between clay platelets and as a free pore water volume. When the sediments are compacted during burial, most of the pore space water is expelled. With further burial there will be increased overburden stress and increase in temperature, which results in the escape of water from the structures between clay platelets into the pore space. This result is the collapse of the clay lattice and in combination with the potassium ions, Montmorillointe is converted to Illite (Rabia, 2005). The Illite packets are typically higher density and form an impermeable layer that prevents further water loss form the rock pore space. This increase of free water in the pore spaces will result in overall formation pressure increase as these pore fluids assume part of the overburden stress.

Aqua thermal pressuring is another mechanism that leads to the increase in pore pressure. One can easily see that a tin can containing water will eventually pop its lid when placed over a fire. Similarly, when fluids in the pore spaces of buried rock are subjected to increased temperatures, the result is an expansion of the fluid molecules and thus an increase in pressure against an impermeable seal. The point of most contention regarding aqua-thermal pressure is not the generation of pressure but the holding of the seal (Hillier, 2000).

Over pressure can also result from the generation of hydrocarbons in the pore space of rocks. This is particularly true if the rate of hydrocarbon generation (fluid volume increase) is greater

than the rate of fluid expulsion or loss. Hydrocarbon generation results from the transformation of high-density organic substances (kerogen) to lower density fluids such as Oil and Gas. This process is dependent on the Kerogen type, quantity of organic material, thermal window and rock permeability (Guo, 2010).

1.3 Motivation

The petroleum exploration industry spends upward of $20 million dollars per well on drilling costs associated with over-pressured formations, while worldwide expenditure estimates are in the vicinity of over $1.08 billion per annum (Dutta *et al.,* 2002). Since drilling high pressured formations is unavoidable in many cases and even applies to legitimate targets of exploration, a better method for predicting pre-drill formation pore pressure is necessary. Traditional research has focused on using an empirical relationship between seismic velocity and pore pressure to predict formation pressure (Doyen et al., 2004). Other investigators have shown the sensitivity of seismic velocities to other factors such as lithology and pore fluid content, thus reducing the reliability of purely velocity based methods for pore pressure prediction. In recent years, new approaches based on seismic attributes and acoustic wave absorption have been developed and patented. These methods utilize the relationship between seismic wave attenuation and overburden stress (Young & Lepley, 2005)

The objective of my study was to focus on techniques that combine seismic attributes with advanced pattern recognition software to predict pore pressure in the lower Paleozoic Qalibah formation of northwestern Saudi Arabia. The pattern recognition software used in this study is called Support Vector Machine (SVM). SVM classifies data based on a separation margin between types of data and is based on statistical adaptation and learning theory. Researchers have shown from tests on actual 3D seismic data that SVM is able to accurately predict

reservoir properties from the computed seismic attributes (Jaikang et al., 2004). The final result of using the SVM algorithm will be quality controlled, the algorithm's parameters adjusted, and the process iterated with various types and classes of attributes to arrive at the "best" combination of well and seismic attributes that can reliably predict the formation pore pressure.

1.4 Previous work

There are not many reports regarding the utilization of seismic attributes for the prediction of abnormal pressure in the sediments of Northwest region of Saudi Arabia. Shaohua Zhou et al. (2009) studied central Ghawar Jilh Formation over pressure and its prediction using integrated 3D pore pressure modeling software (PP3D), which utilized geological, logs and drilling reports in the area of interest (non-seismic methods). Al-Mustafa and others studied the utility of Supervised Vector Quantization (SVQ) and Unsupervised Vector Quantization (UVQ) analysis of acoustic impedance and its Fourier transform attributes to map the distribution of over pressured rocks in the base Jilh sequence of Uthmaniyah Field in Saudi Arabia (Al-Mustafa, 2001). More recently and in the same area as this study, Daniel Mujica and others (2012) conducted a feasibility study to predict formation pore pressure using a residual normal move out (NMO) 3D seismic volume computed from Pre-stack Time Migrated (PSTM) gathers. This method used amplitude verses offset (AVO) techniques and well data in the area of interest is used for calibrating the interval velocities and densities (Mujica, D et al, 2012)

The result of this study indicated that seismic attributes with data driven neural classification methods can yield meaningful results in identifying areas of high pressured rocks, which has encouraged the current study. Many other industry studies have been carried out using mainly seismic velocities and well data to predict formation pressure. These studies are local in nature

and the researchers have reported some success in using the results of their pressure prediction studies in their local areas.

There are some laboratory tests, covering the entire seismic frequency range, that have shown a strong empirical relationship between seismic frequency attenuation and formation pore fluid content. A number of researchers have suggested that seismic wave attenuation in dry rocks is minimal, while fluid filled rocks exhibit strong frequency-dependent attenuation (Spencer, 1981). It has also been observed that in most natural earth-materials, seismic wave attenuation increases with frequency and that the high-frequency components are attenuated more strongly than the low-frequency components. My research will review the literature on this empirical relationship and propose a methodology that can reliably predict formation pore pressure from seismic attributes.

CHAPTER 2

GEOLOGICAL SETTING OF STUDY AREA

2.0 Northwest Arabian Basin

The study area is located in the Nafud Basin of Northwest Saudi Arabia. The Nafud Basin is part of a larger plain that has an area of over 375,000 km^2, covering roughly an eight of the Kingdom of Saudi Arabia and has an average present day elevation of approximately 900 meters above sea-level (Vincent, 2008).

Figure 4 : Location of study area. Google maps 2012

The Nafud Basin area is bounded on the west by the Al-Jawf graben system, to the south by the Arabian Shield and to the north by the Palmyra fold belt of Syria. This basin was part of a vast stable region in Paleozoic time which extended into Northern Africa. This is a geologically complex platform that has been subject to rifting, volcanism, many episodes of inversion, and partitioning. Throughout the basin, thick sequences of Paleozoic clastic sediments with some minor carbonates have been deposited extensively during Cambrian to Devonian. These sediments thicken significantly to the northeast and there is evidence of the Hercynian erosion removing a considerable amount of sediments to the northwest (Aoudeh, 1994).

The Al-Jawf Graben, which is a northwest-southeast trending failed rift, is also located in the Nafud basin. The Graben is part of an Infra-Cambrian system that has been subjected to several episodes of tilting, swelling, and rifting including during Hercynian time.

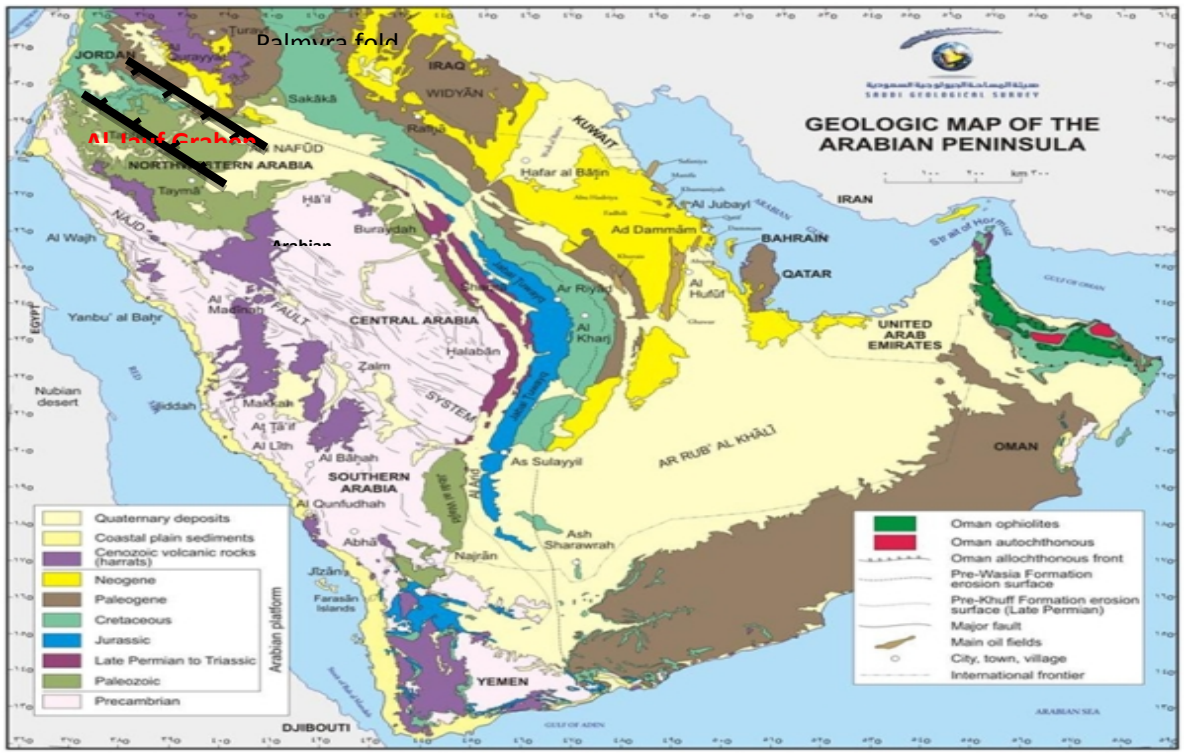

Figure 5: General Geological map of the Arabian Peninsula. Modified from Saudi Geological Survey

During early Paleozoic, the Arabian part of the north Gondwana super continent was located in close proximity of the South Pole (Figure 6). This resulted in the deposition of widespread glacial sediments and sea level rise and fall causing regression and transgression of the ocean floor around Gondwanaland. The duration of the glaciation period is approximately 0.5-1.0 million years, which significantly affected the sedimentary strata (Liining, 2000). The glacial sediments are dominated by thick sandstones and diamictites including glacially curved paleo-valleys and channel fills.

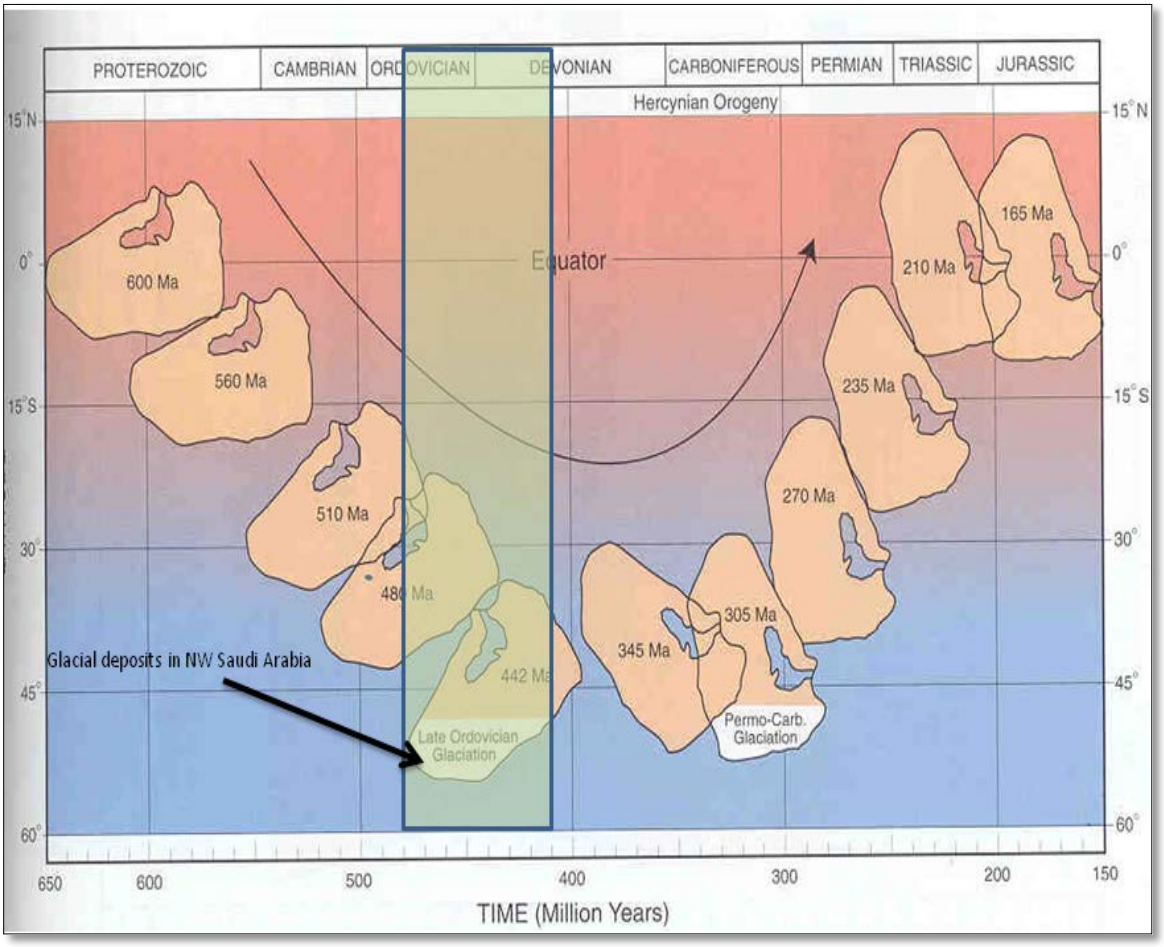

Figure 6 : Arabian plate through time

The early Paleozoic sediments outcrop in three areas in Saudi Arabia (see green shaded areas in Figure 5): In the Northwest near the town of Tabuk, extending to the west to Jordan, in Central Saudi Arabia near the localities of Hail and Qasim and in the south of the country from Jabal Wajid area to Yemen (Vaslet, 1990). For the purpose of my research, I will describe the Paleozoic sediments in three general categories. One is the Cambrian to Mid-Ordovician pre-glacial sediments; followed by the Late-Ordovician Glacial deposits and the third is the overlying Silurian Shale strata that are over pressured and the focus of this study.

2.1 Lower Paleozoic Pre-glacial Sediments

During the Upper Cambrian to Lower Ordovician, increased influx of siliciclasitc deposits terminated the carbonate sedimentation in the Arabian plate. This resulted in the deposition of siliciclasitc apron conformably over the Middle Cambrian strata. Fluvial to fluviodeltaic to shallow-marine environments persisted in the Northern localities of the Arabian plate. These fluvials grade into distal shale-dominated marine environments toward the east in Zagros (Konert, 2001).

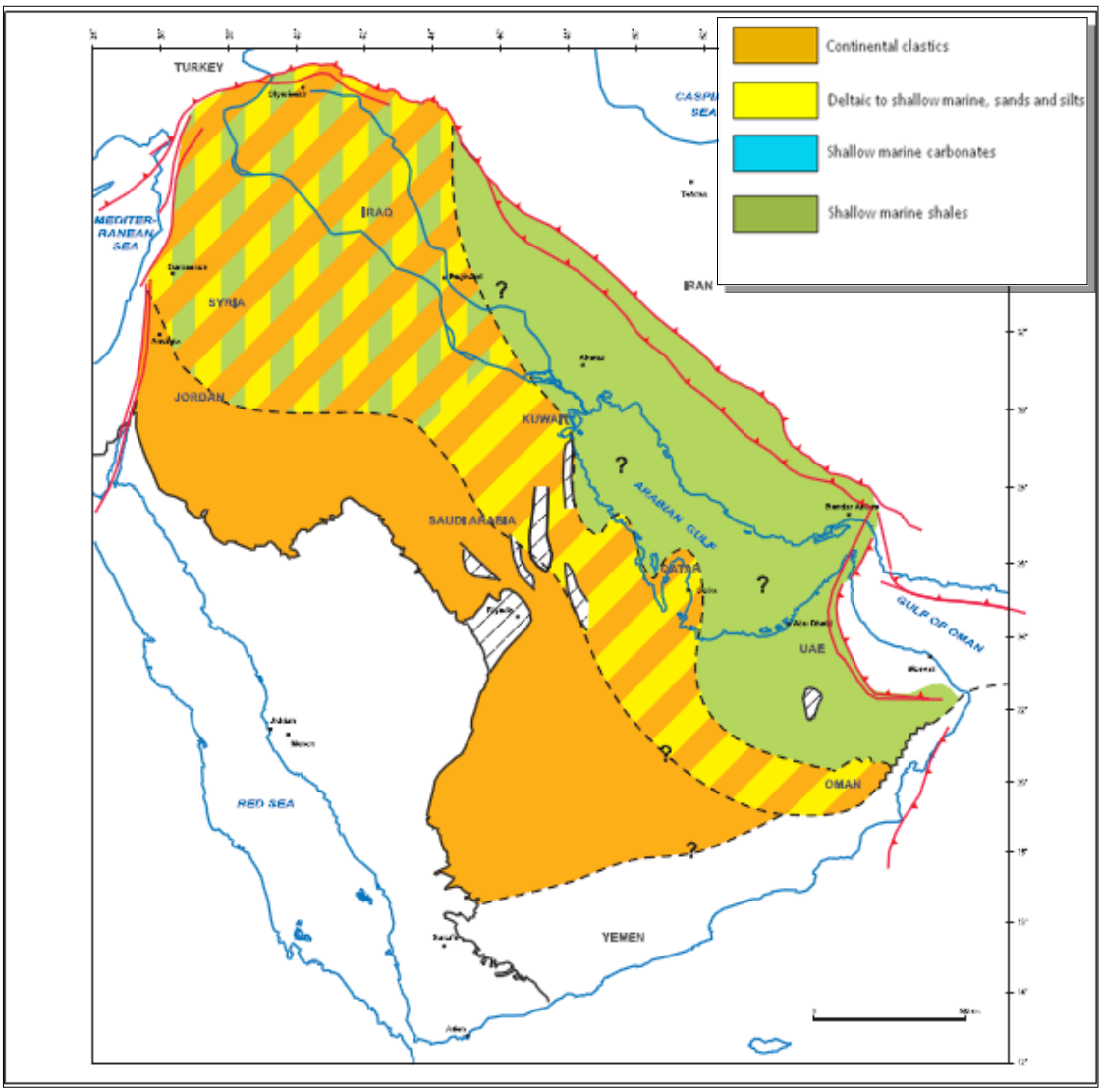

Figure 7: Late Cambrian depositional environment (Konert, 2001)

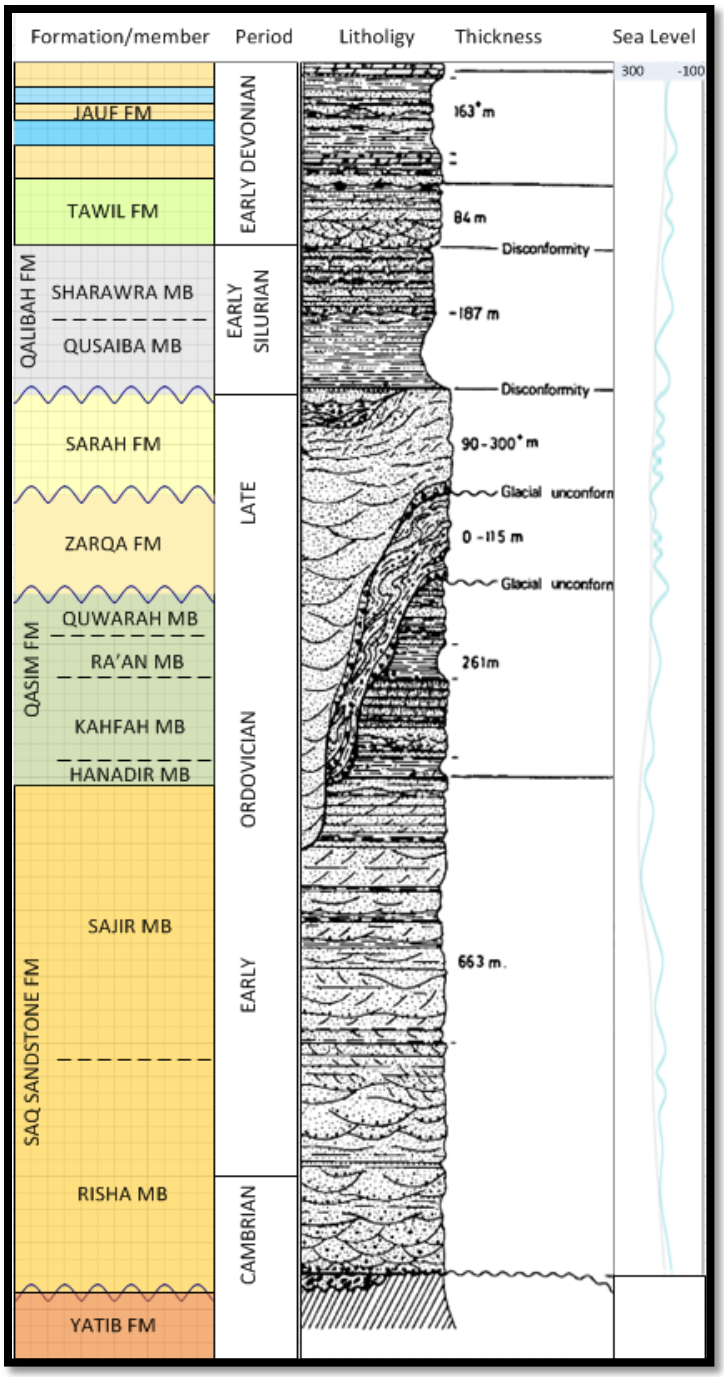

Figure 8: Generalized stratigraphic column (Cambrian-Devonian), Northwest Saudi Arabia (Modified after Vaslet, 1998)

The Pre-glacial deposits are the sequence of strata deposited below the earliest unconformity, before the first glacial episodes and range in age from Cambrian to Late Ordovician. This sequence is represented by the Tayma Group which has three members: Yatib, Saq and Qasim Formations.

The Yatib Formation, which unconformably lies on top of the Proterozoic basement, is mainly deposited in low relief paleosurface of the Arabian Shield and is primarily composed of coarse grained sandstone and siltstone set in an arenitic matrix and polymictic conglomerates (Vaslet, 1990).

Overlying the Yatib is the Saq Sandstone Formation, which is of Cambrian to Early Ordovician age. This formation is subdivided into two members; the Risha Mebmber and the Sajir Member. The Risha Member is deposited unconformably on Proterozoic Shield sediments. The upper part of the Risha is composed of coarse to fine grained sandstone. The lower part is mainly conglomerate of centimeter-sized, well rounded, white quartz pebbles in a sandstone matrix. This member is interpreted as braided alluvial deposits that grade upward into a deltaic system. The Sajir Member is about 355 meters tick in the upper part of the Saq Sandstone Formation and represents a pro-deltaic shallow water environment deposit. It is characterized by medium-to-fine grained sandstone and contains *Cruziana* trails and Scolithus bearing sandstone in the topmost part (Vaslet, 1990).

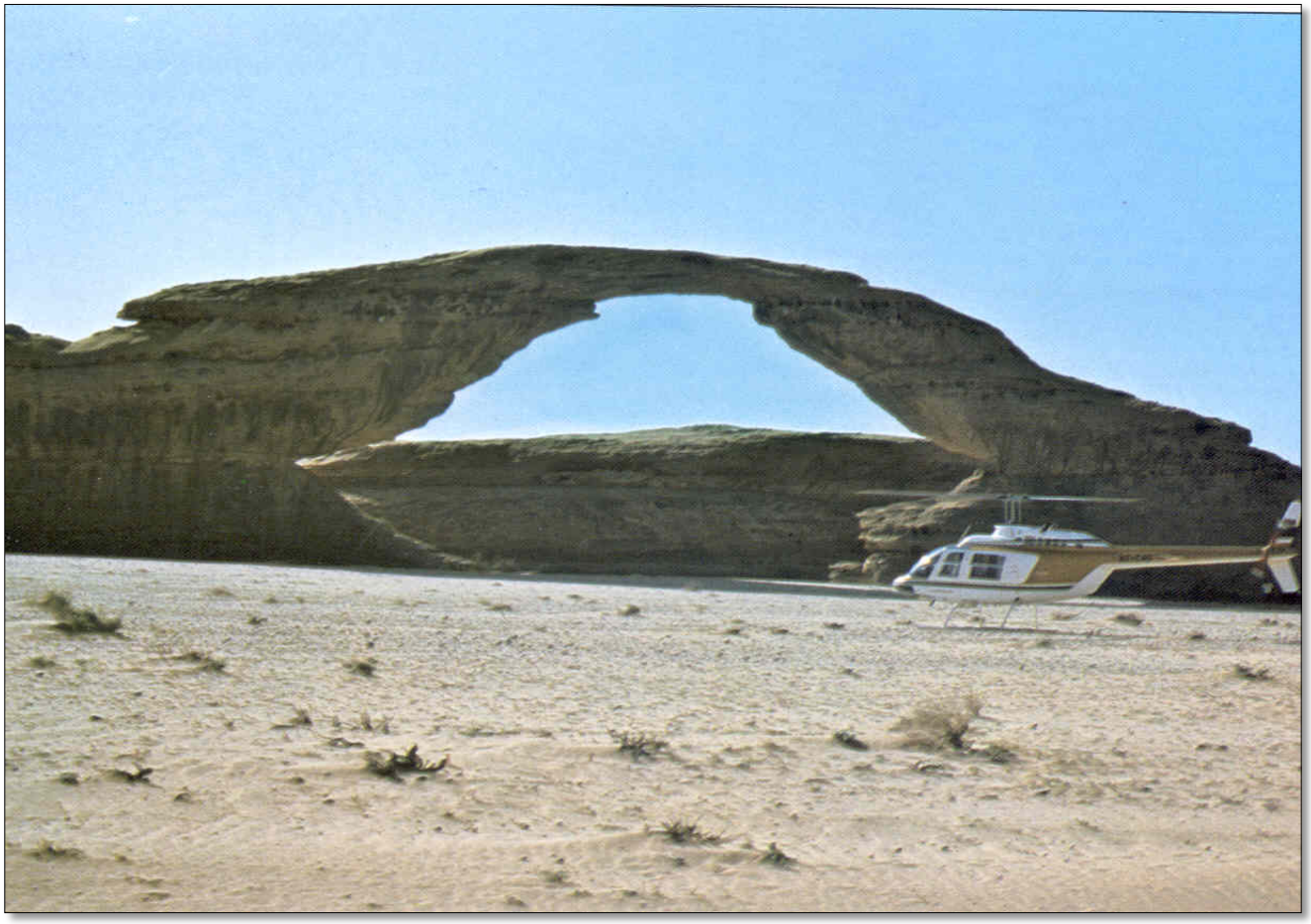

Figure 9: Saq Sandstone Formation Outcrop in Jabal Saq, Saudi Arabia (Dr. Hariri Regional Geology notes KFUPM)

Lying conformably on the Saq Sandstone Formation is the third Formation of the Tayma group, the Qasim Formation. The type section of this formation is in the Qasim region of central Saudi Arabia and is of Llanvirnian to Caradocian age and has a total thickness of 261 meters. The topmost member of the Qasim Formation is the Quwarah member, which is approximately 87 meters thick as described by Willams et al 1986. This member is characterized by alternating fine-grained sandstone, micaceous siltstone and claystone, and is recognized to be Caradocian to Ashgillant in age. The Quwarah is truncated everywhere by base of Zarqa Formation, which is the first glacial erosional surface in the region (Vaslet, 1990).

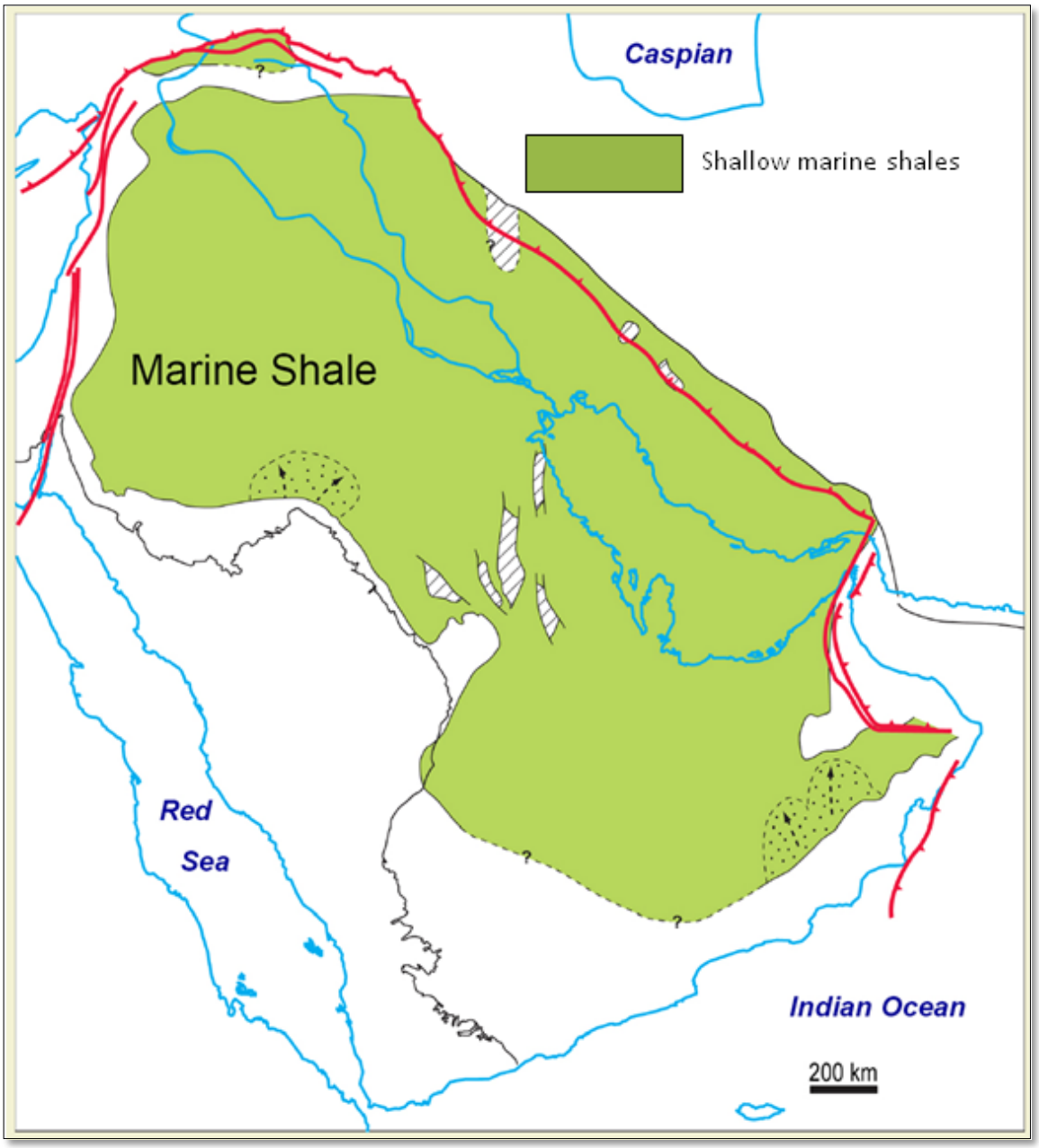

Figure 10: Middle Ordovician, middle to outer neritic shale deposits over most of the Arabian Plate (Konert 2001)

The boundary between Middle to Lower Ordovician is marked by a wide spread deposition of middle to outer neritic shales in the Arabian plate (see Figure 10). This is a maximum flooding surface of Llanvirian age and is found throughout the basin. In some localities the shale is organic rich which is a characteristic of restricted water circulation in the basin. The Middle Ordovician strata are a result of inner neritic to estuarine or deltaic environmental deposits. This is followed by a transgressive cycle of Caradocian age (Konert, 2001).

Below the Quwarah Member of the Qasim Formation, is the 45 meter thick Ra'an Member as described by William et al, 1986. This member contains basal graptolite and trilobite fauna that is of late Caradocia age, with mainly outer-shelf environment claystone deposits (Veslet, 1990).

Below the Ra'an member is the 104 meter thick, Kahfah Member as defined by Vaslet and others, 1987. There are two assemblages of this member; the upper assemblage is a 64 meter thick unit that consists mainly of fine grained tigillite-bearing sandstone of marine origin and deposited in a prodeltaic environment. The lower section is about 40 m thick section and made of fine-grained feldspathic sandstone interbedded with claystone bearing graptolite and trilobite of possible Llandeilian age. In some localities it contains bioclastic sandstone. (Vaslet, 1990).

The bottom most member of the Qasim Formation is the 26.5 m thick, Hanadir member and contains graptolite, trilobite and conodont fauna of middle to late Llanvirnian age (*Didymongraptus murchisoni Zone*). Vaslet describes the base of this member as phosphatic, bioclastic (fish debris) conglomerate and defines it as showing

clear transgressive character and possible hiatus of early Llanvirnian section between the Saq and Qamsim formations (Vaslet, 1990).

2.2 Late Ordovician Glacial Sediments

The second category of succession is the glacial deposits marked by the Late Ordovician glaciation of Gondwana. During late Ordovician period, sub-Saharan Africa was covered by a polar icecap, which advanced into Northwestern Arabia (Figure 6) and resulted in the deposition of two distinct episodes of glacial strata. These sequences are composed of tillite and proglacial siliciclastics, mostly sandstone in incised valleys adjacent to the Arabian shield and Southern Jordan (McClure, 1978, Vaslet, 1987, 1990).

The Middle Ordovician glacial deposits formed a deep incised valley system reaching depths of over 500 m. These incised channels can be recognized in subsurface seismic data of northern Saudi Arabia. This also resulted in the fall of relative sea-level causing the influx of fluvial to deltaic sands on top of the deeper marine sediments in parts of the Arabian plate (Konert, 2001).

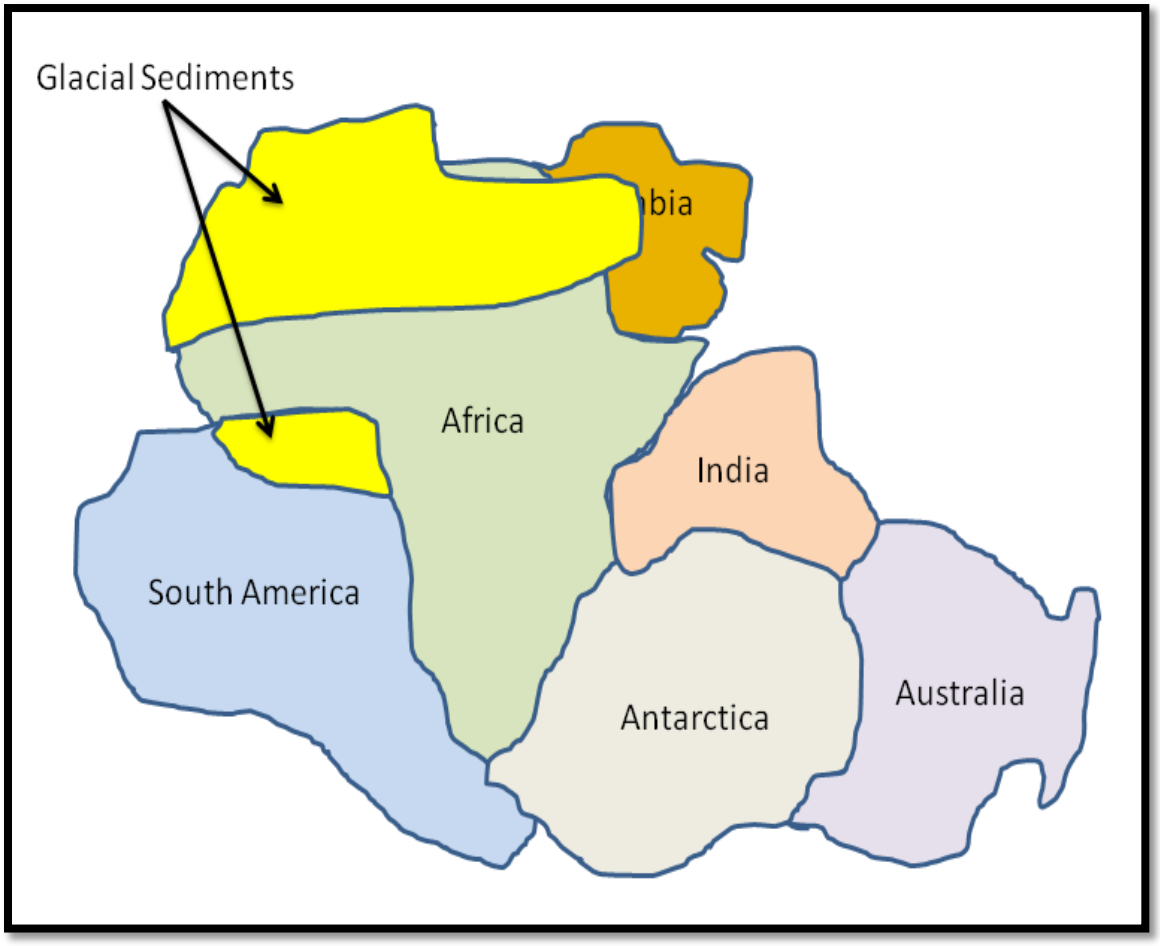

Figure 11: Upper Ordovician continental configuration and location of glacial deposits (After Abed, 1993)

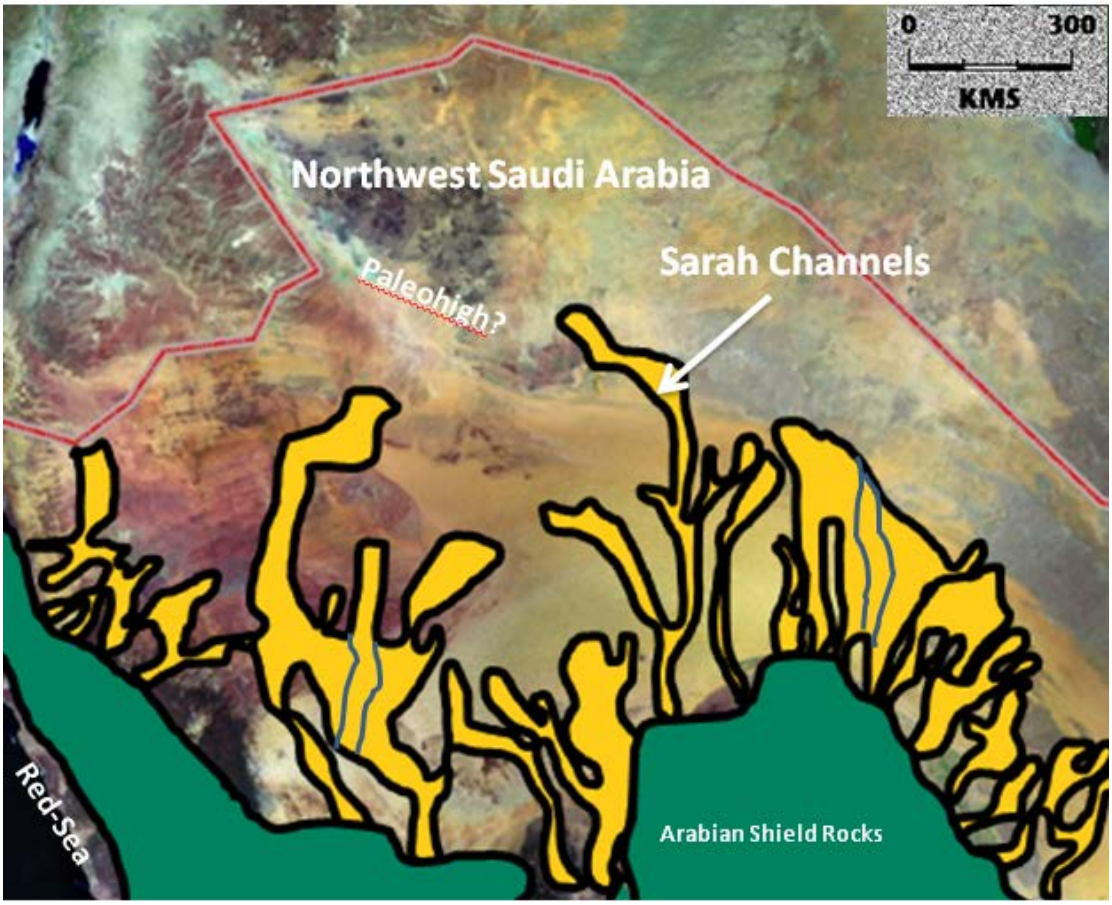

Figure 12: Distribution of glacial channels, Northwest Saudi Arabia (Modified after Aoudeh, 1994)

Vaslet and others (1990) describe the subdivision of the upper Ordovician glacial sediments in Northwest Saudi Arabia into two formations: the Zarqa formation and the Sarah formation. Both of these formations are bound by strong glacial unconformities. Both formations have similar composition of tillite, fluvial glacial Sandstone, and glacial marine and lacustrine sediments. These deposits are separated from the underlying Qasim formation by unconformity, however, the paleo-erosion surface cuts down deeply and even as far below as the Saq Formation as illustrated in Figure 13 (Vaslet, 1990).

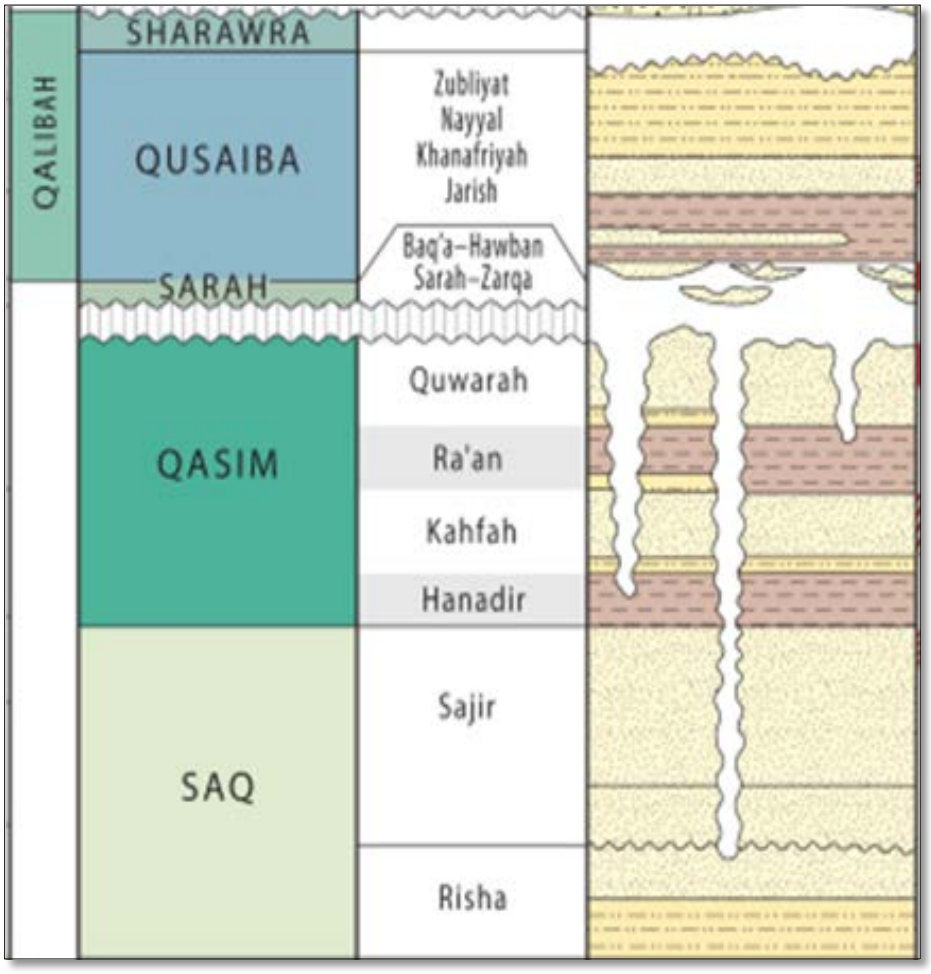

Figure 13: Stratigraphic chart showing glacial deposits cut deep into underlying Formations

As defined by Vaslet, 1987, the type section of the Zarqa formation is located in the vicinity of Jal Az Zarqa. This Formation is 115 meters thick and is composed mainly of interbedded siltstone or clayey siltstone, large clay boulders, fine-grained micaceous sandstone that usually is slumped, and tillite. There are a number of discontinuous outcrops of the formation and the most complete outcrop site is located in central Saudi Arabia near the town of Asnyah. Zarqa Formation erodes and unconformably lies on top of the Qasim Formation, resulting in its deposition in the channels created by the erosion of the Qasim Formation. Formation outcrop evidence shows that the Zarqa deposits are located in the low-lying zones of a paleotopography, notched into the Qasim Formation. The traces of the paleovalleys are visible on the surface (Vaslet, 1990).

The second formation of the Late Ordovician Glacial sediments of Northwest Saudi Arabia is the Sarah Formation. This formation is deposited in deeply cut glacial channels of the substratum. Due to secondary cementation that hardened the porous material, these paleovalleys are seen as a topographic high in present day topography.

The Sarah Formation is composed of homogeneous medium grained, cross-bedded sandstone that is of fluvial origin. Layers of continental glacial debris are interbedded with the sandstone and in some paleovalleys, the bottom part of the strata show striated glacial floor. This shows the effect of ice activity when the formation was being deposited in the paleovalleys. The upper section of the Sarah Formation is composed of sandstone that overflowed the paleovalley channels and covered much of central Saudi Arabia. This sandstone cover is not strictly glacial and included sandy sediments that were released from melting ice sheets and mounts. The very top portion

of the Sarah Formation is the Hawban Member, which is indicative of a new glacial episode characterized by *roches moutonnées* and other glacial sediment indicators. These sediments are increasingly marine in origin and may represent a final ice cover of the Arabian plate after the deposition of the Sarah Formation and before the return of the prevalent marine environment (Vaslet, 1990)

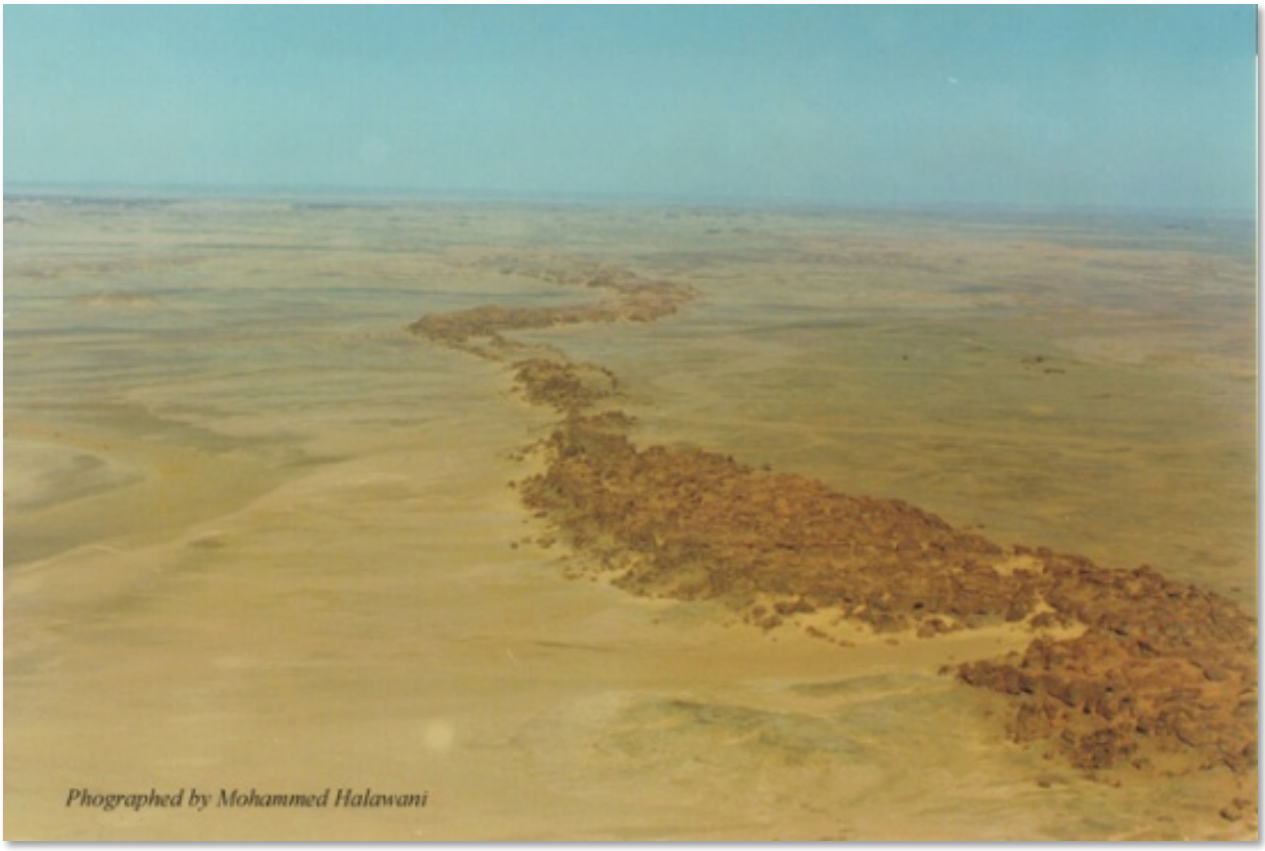

Figure 14: Aerial photograph showing present day surface topography of the glacial sediments

2.3 Post-Glaciation Silurian Deposits

The third, and the focus of my study, is the Silurian, transgressive marine deposits that disconformably overly the glacial deposits. The early Silurian period was characterized by major global warming, which caused the contraction of the glaciers. This resulted in a rapid sea-level rise that flooded most of the Arabian plate and deposited a layer of shallow marine sediments (Fig 14) (Konert, 2001). Shallow-to-open-marine environments are prevalent on the Arabian platform during this time. Some areas are covered by anoxic waters that lead to the deposition of the prolific Silurian "hot" shale. These initial deposits are followed by a thick cover of shale and sandstone. These sediments are represented by the Qaliba Formation, which is separated into two members; the lower member is the Qusaibah Member, consisting of predominantly clayey shale, interbedded with siltstone. The upper section of the Qaliba Formation is represented by the Sharawra Member, which is mainly composed of marine sands with thin conglomerate layers at the base (Vaslet, 1990).

The Qusaiba Member, also known as the Qusaiba "Hot Shale" is the source rock of over 90% of the Paleozoic hydrocarbons found in the region and also is a seal to the underlying Ordovician reservoirs (Aoudah et al, 1994). Researchers such as Aoudah et al also contend that during the Silurian, the Al Nafud basin was divided into two main sections, one is the Tabuk-Tayma embayment and the other is the Ar'ar Al-Jawf sub-basin. It is postulated that this subdivision of the Al-Nafud basin is often masked by the tremendous thickness of the shale unit deposited in the basin. When the isopach of thin layers such as the Base Qusaiba Shale is mapped, a new picture of the basin is revealed. The "Hot shale" isopach shows the Al-Jawf graben as a paleohigh that

separates the western and eastern sides of the basin. The isopach thickens tremendously to the east and west attaining thickness that reaches drilled depths of 175 feet at Tayma to the west and possibly over 300 feet to the east, into Iran (Aoudah, 1994). The Eastern sub-basin extends from Northwest Oman to the north of Bandar Abbas in Iran, while the Western sub-basin extends from North Africa to North East Saudi Arabia and most likely to the western provinces of Iran (Bordenave, 2002).

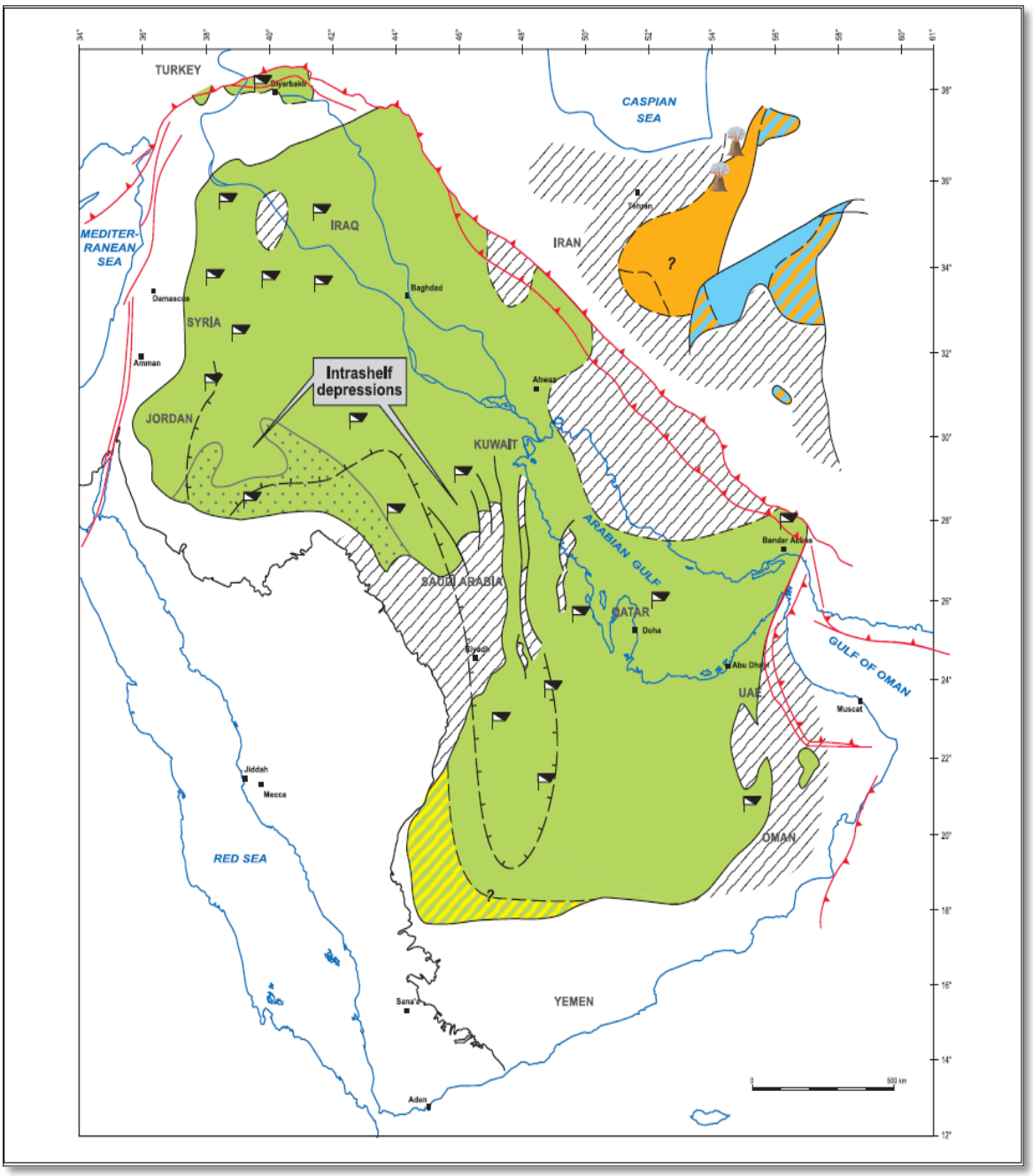

Figure 15: Map showing depositional extent of Early Silurian sediments (Konert 2001)

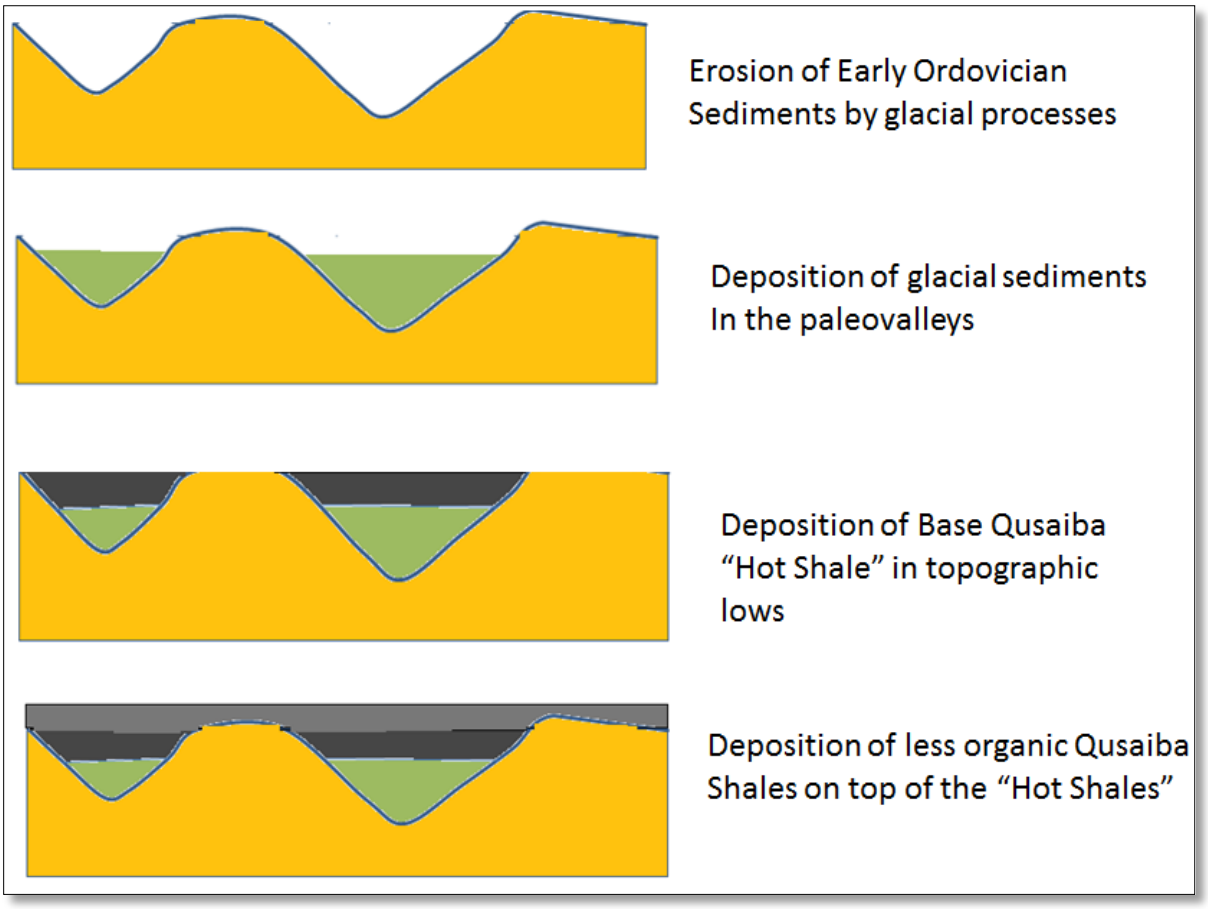

Figure 16: Simple model showing Qusaiba "Hot Shale" sediments

2.4 Base Qusaiba Depositional Model

Subsequent to the end of the late Ordovician glacial event, sea-level rose due to the rapid melting of ice, resulting in a wide spread eustatic sea-level rise and transgression toward the south. This has been a rapid transgression with low sediment content and in the early stages of the transgression, only lower relief areas where flooded and shales deposited (Fig 15). The earliest Silurian deposits in Africa and Arabia are those of organic-rich shale units. Ultra-organic-rich shales were deposited during this short time period and on top of this organic-rich layer, are lean, less organic shales (Luning, 1999).

The Qusaiba shale formation is a thick unit composed of substantial, dark gray shale that occurs widely throughout the Middle East. In Saudi Arabia, this unit outcrops in three localities (Fig 16); namely Qasim/Tabuk in the Northwest, Central area, Qusaiba and in the Southwest Wajid belt. (Aoudeh, 1995).

At its type section, the Qusaiba Member contains 256 m of organic-rich, layered shale. The lower part of the unit is characterized by numerous graptolites and has interbedded, rippled siltstone, and micaceous siltstone and sandstone in the upper part. There is a gradational contact between the Qusaiba and the overlying Sharawra Member (Mahmoud et al, 1992).

Mahmoud et el (1992) describe the subsurface of the Qusaiba Member in Saudi Arabia using Saudi Aramco well ST-39, which was drilled in the central part of the country. They show this well to have a complete and extremely thick Qusaiba section and partial Sharawrah formation due to local erosion as a result of Hercynian and younger

events of structural deformation. These researchers also use Saudi Aramco Udaynan-1, as a reference section, as this well has a complete Sharawrah Member and together with ST-39 shows a complete section of the all members of the Qalibah Formation. The location of these wells is indicated in Figure 16.

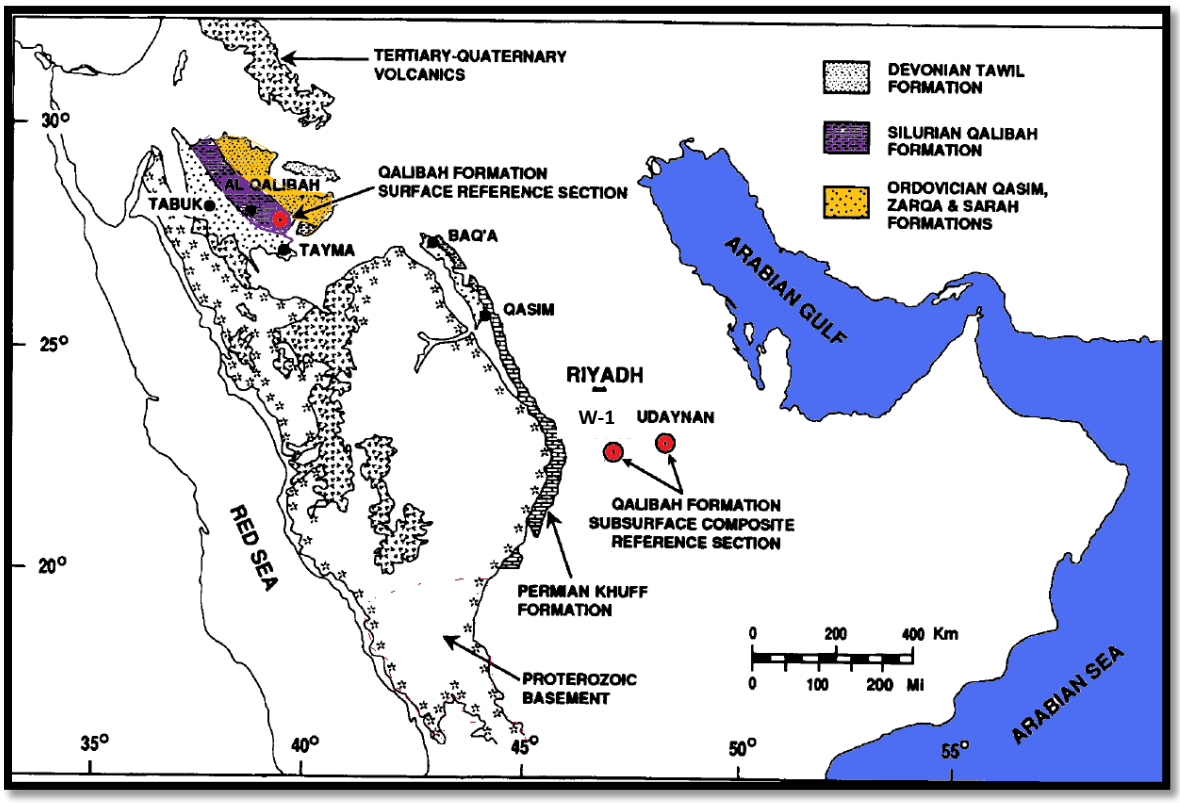

Figure 17: Location of surface and subsurface type section of Qaliba Formation (Modified after Mahmoud, 1992)

In the W-1 well, the Qusaiba is 603 meters tick and is composed of mainly laminated to well-bedded alternation of siltstone and gray to black micaceous shale. The Qusaiba "Hot Shale" is shown to be in the lower 70 meters of the W-1well. This section exhibits sharp increase in gamma radiation typical of many organic-rich facies (Fig 17). The Qusaiba shale is also characterized by overpressure conditions that may have resulted from hydrocarbon generation within the formation and surrounding beds, forming a bounding seal against hydrocarbon migration (Faqira et al., 2010).

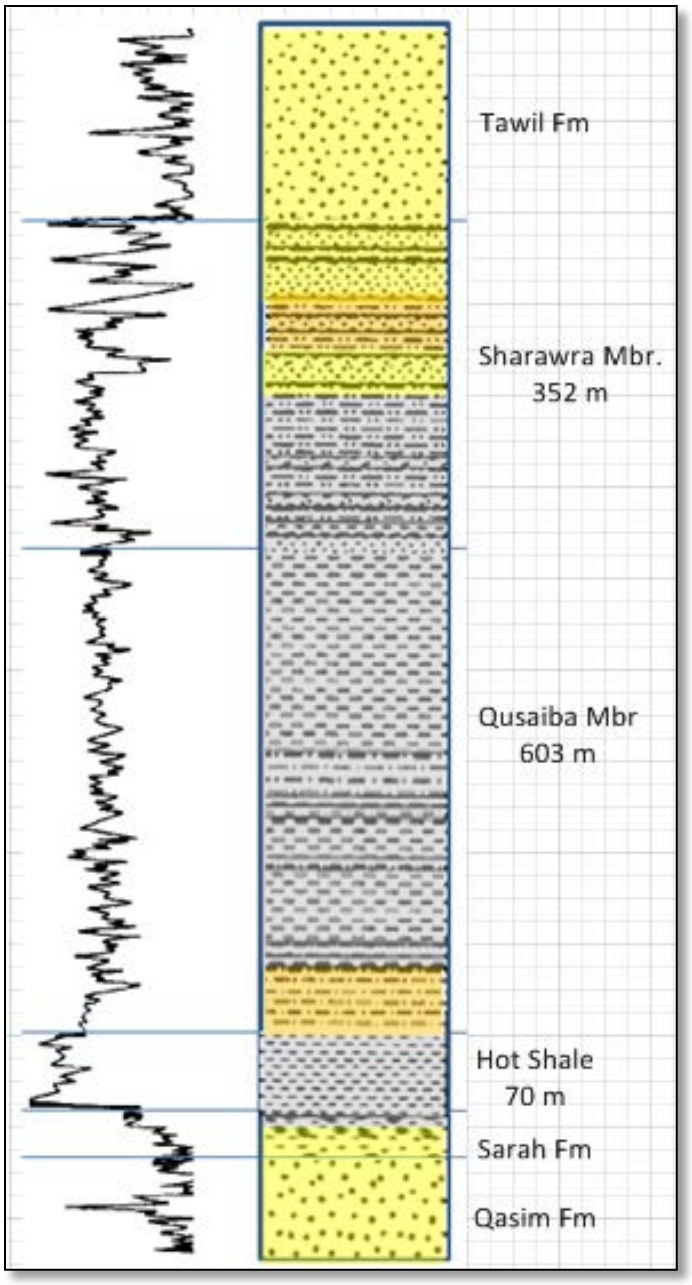

Figure 18: Composite log reference section of lower Qalibah Formation from wells in Central Arabia (Modified after Mahmoud et al, 1992)

CHAPTER 3

COMPUTED SEISMIC ATTRIBUTES

3.0 Introduction

Seismic attribute is defined by Sheriff (1991) as a measurement derived from seismic data. This general definition includes AVO analysis, inversion, interval velocity, pore pressure prediction, reflector terminations, complex trace attributes and countless computations resulting from seismic data.

The use of seismic attributes can be dated back to the early 1960s when Russian researchers Churlin and Sergeyev reported the use of seismically derived measurements to directly detect hydrocarbon reservoirs. This was done before the availability of digital recording equipment, so the quality and usage of these measurements were limited. The availability of digital recording technology and color seismic displays in the early 1970s has provided a tremendous advancement in the usage, generation, interpretation and preservation of seismic measurements, such as

relative amplitude for bright-spot detection and pay-sand thickness. The advent of seismic inversion techniques to convert post-stack seismic amplitude data into impedance volume in the late 1970s also provided a significant value of generating seismic attributes. One could gather crucial reservoir properties such as lithology and porosity directly from the acoustic-impedance attribute volumes.

The use and generation of many types of seismic attributes have become widely used in the industry in the 1980s. Also, many of the interval and formation attributes were introduced. These attributes allowed interpreters to generate seismic measurements representing the average quantity of interest between two picked horizons and a window centered on a given reflector. The use of seismic attributes has grown tremendously since then and recently almost all seismic interpretation results involve the use of seismic attributes of one kind or another (Chopra and Marfurt, 2007).

In current times, no interpretation would be considered complete without various structural and stratigraphic seismic attributes that augment the geological and geophysical interpretation results. The tremendous growth of seismic attributes has also sparked the growth of automated pattern recognition systems. The early seismic attributes were designed for the perception of human eye; however, many scientists have recognized that the combination of multiple seismic attributes into a coherent system could be a powerful interpretation tool. This caused the development of automated pattern recognition algorithms to find meaningful relationship of extracted information for the huge seismic data set that has been computed from conventional seismic surveys (Chopra and Marfurt, 2007)

Most of the industry standard software has the capability to compute seismic attributes. I will utilize the following seismic attributes for my research in predicting over-pressured formations.

3.1 Instantaneous Frequency

Instantaneous frequency is defined as the dominant frequency at a given time and location. It shows both wave propagation effects and depositional characteristics. It is classified as a physical attribute and can be used as an effective discriminator.

$$\mathrm{f(t)} = \frac{1}{2\pi}\frac{d\emptyset(t)}{dt}$$

where f (t) is the instantaneous frequency and $\emptyset(t)$ is the instantaneous phase.

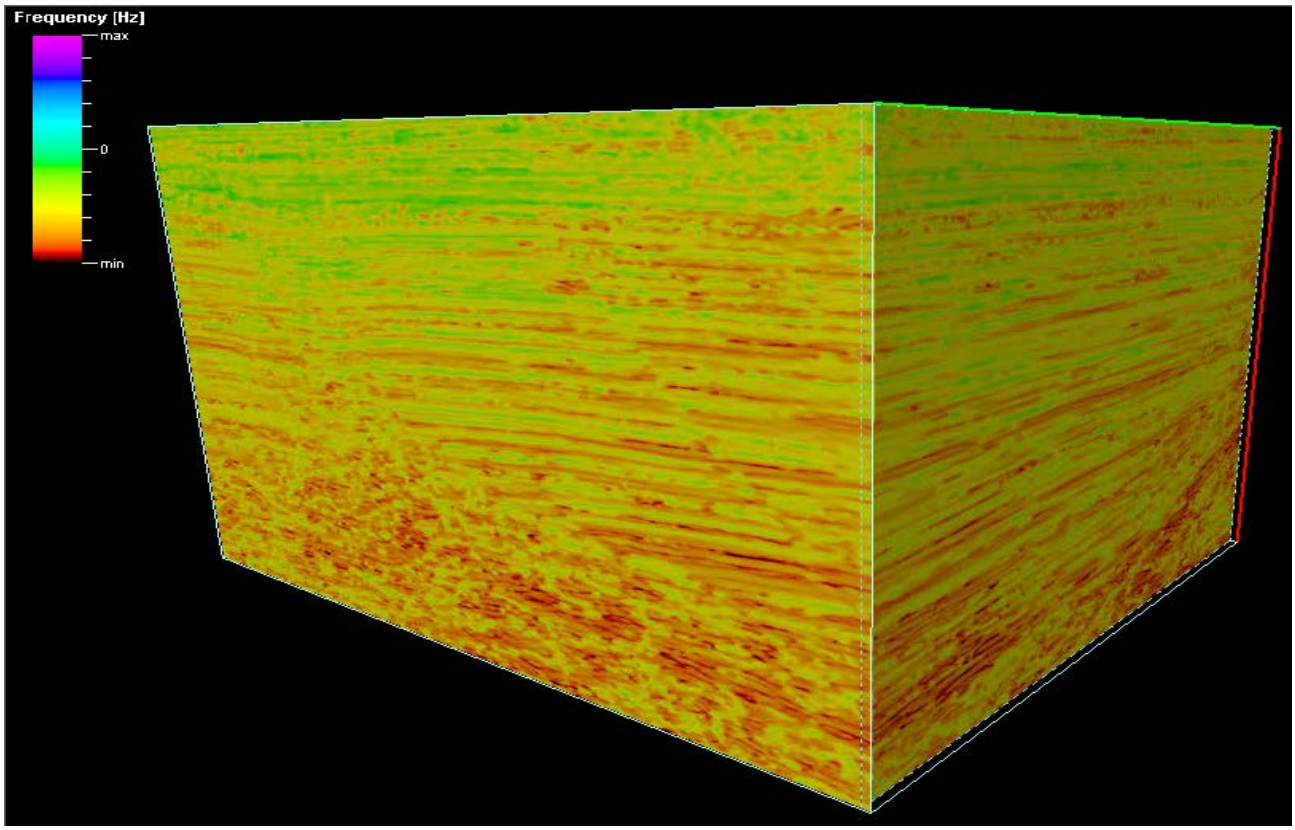

Figure 19: Instantaneous Frequency 3D volume

3.2 Dominant Frequency

Dominant frequency is calculated as the square root of the sum of the squares of instantaneous frequency and instantaneous bandwidth. This attribute, in combination with instantaneous bandwidth, serves as a supplement to the instantaneous frequency, as the three attributes reveal the time varying spectral properties of seismic data and help identify low frequency shadows.

$$fd(t) = \sqrt{f^2(t) + \sigma^2(t)}$$

where:

$fd(t)$ is the dominant frequency

$f(t)$ is the instantaneous frequency

$\sigma(t)$ is the instantaneous bandwidth

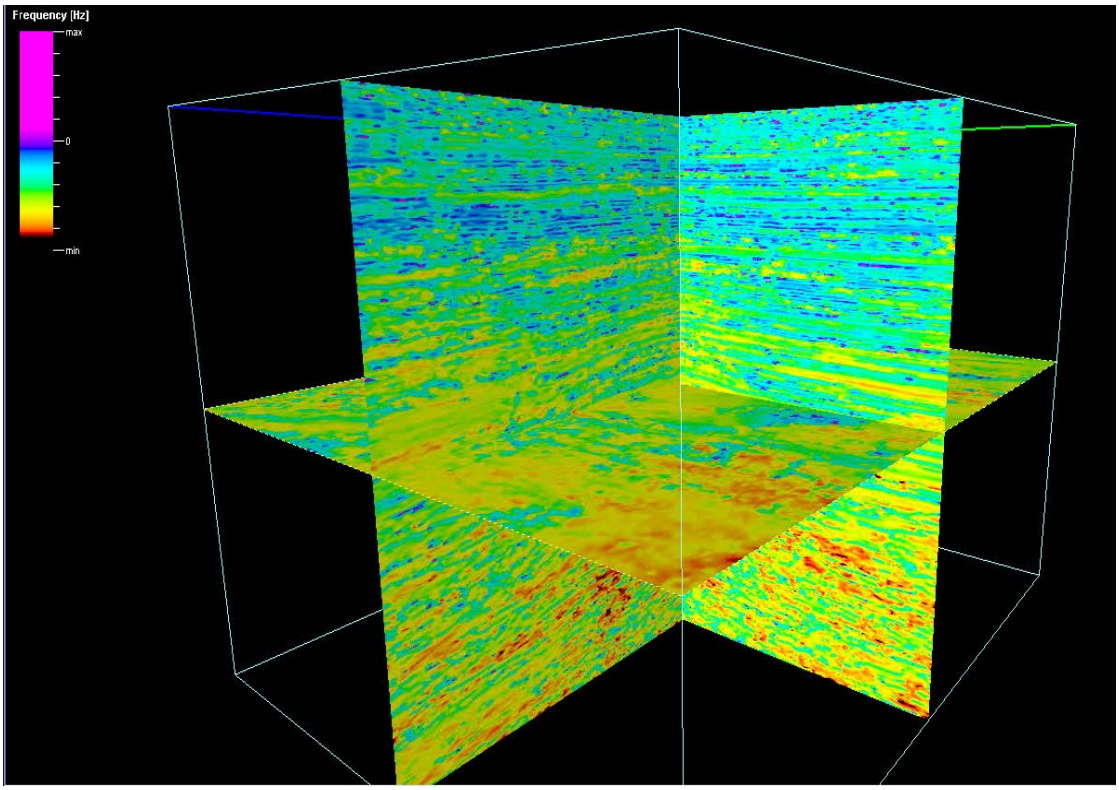

Figure 20: Dominant Frequency 3D volume example

3.3 t* Attenuation

t*Attenuation is the differential loss of high frequencies relative to low frequencies as measured above and below the point of interest. It can be used to identify fracture zones and fluid movement and other rock fluids changes. This attribute is designed to show the type of frequencies (high or low) attenuated in a target zone. The attribute is computed using the following formula:

$$t^* = \frac{\ln\left(\frac{f_{AH}}{f_{BH}}\right) - \ln\left(\frac{f_{AL}}{f_{BL}}\right)}{f_H - f_L}$$

Where:

t^* = t* attenuation attribute

f_H = user defined high frequency

f_L= user defined low frequency

f_{AH} = computed high frequency for given window

f_{AL} = computed low frequency for the given window

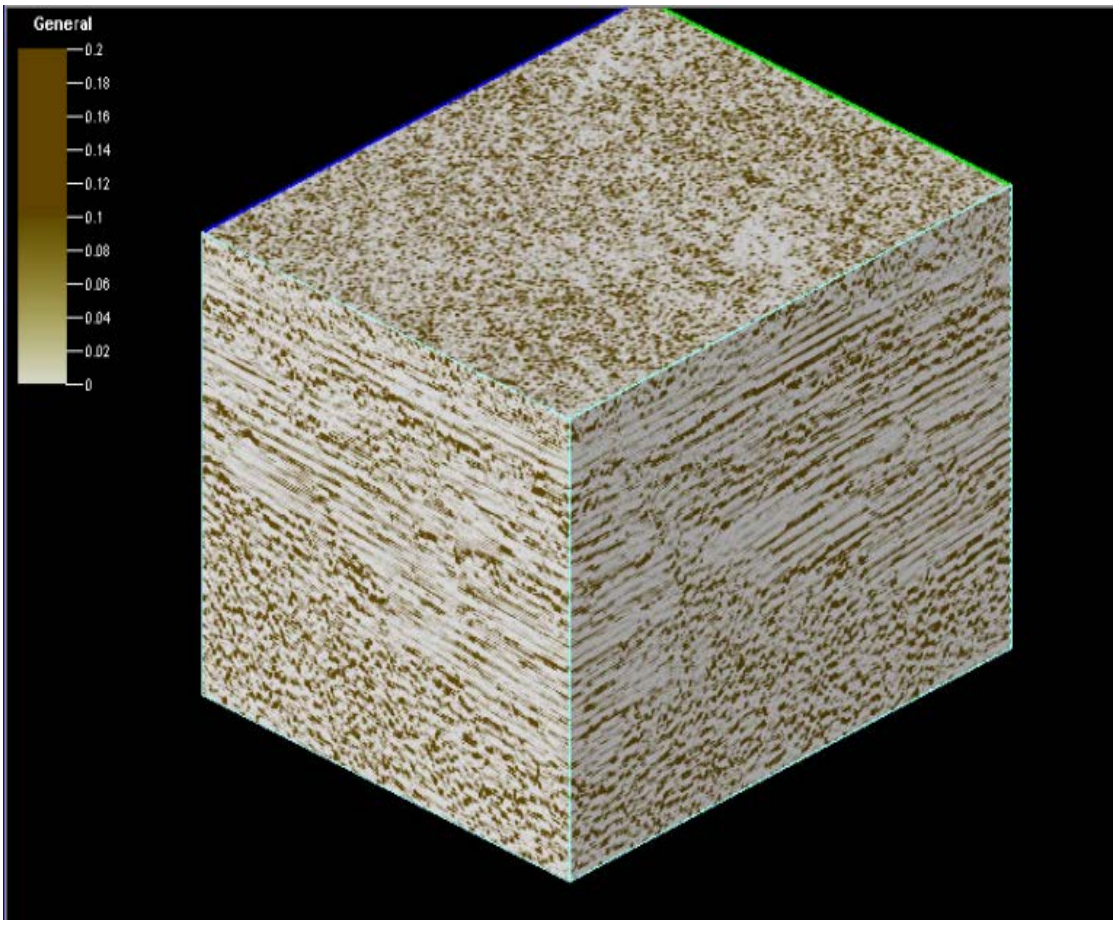

Figure 21: t*Attenuation attribute volume example

3.4 Reflection Intensity

Reflection Intensity quantifies the seismic trace energy and is computed with a moving time window. Reflection Intensity is given by the equation:

$$A_{RI(t)} = \sqrt{1/N \sum_{x \to N/2}^{N/2} |f(t+k)|}$$

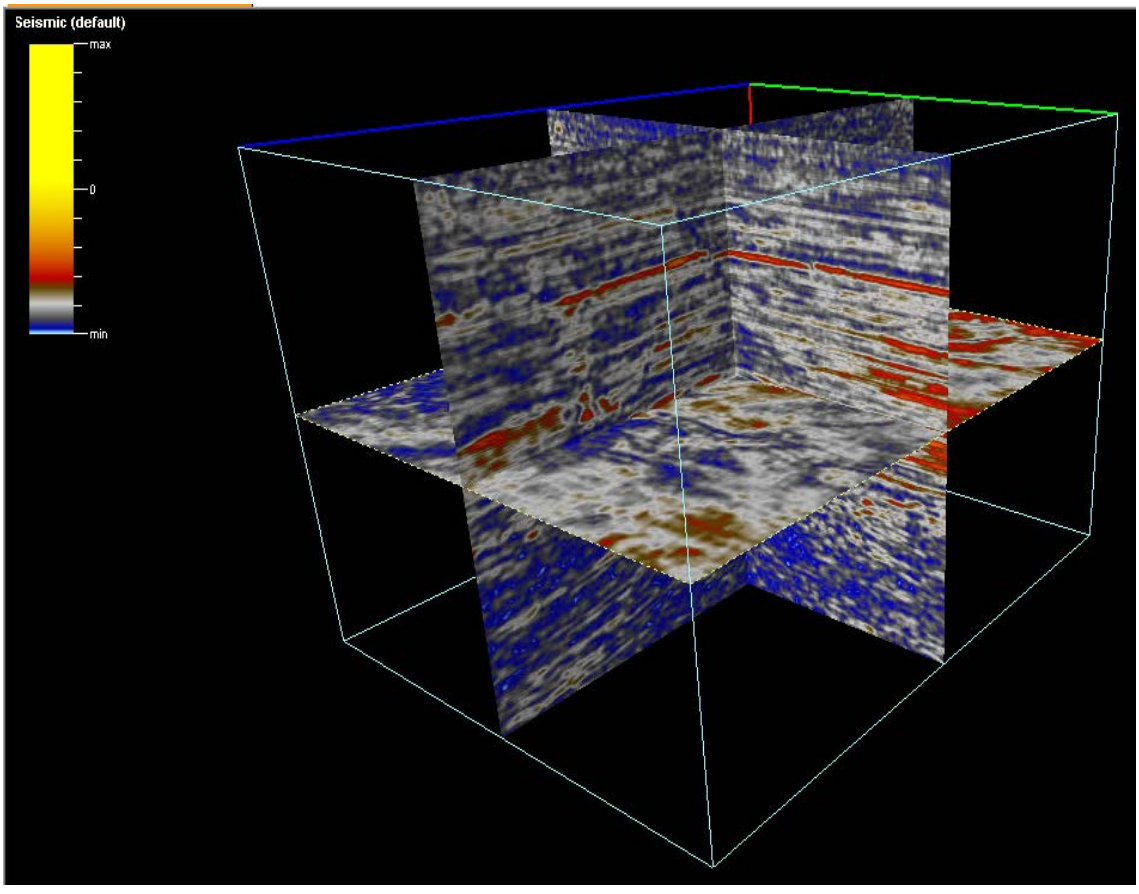

Figure 22: Reflection Intensity 3D volume

Reflection Intensity is useful for delineating amplitude anomalies while retaining the frequency appearance of the original seismic signal.

3.5 Cosine of Phase

Cosine of phase attribute is computed from the cosine of instantaneous phase angle ($\varphi(t)$ and is mathematically computed as :

$$Cosine\ of\ phase = \cos(\varphi(t))$$

The cosine of phase attributes scale the data between values of -1.0 to 1.0 and thus does not contain any amplitude information. This effect enhances reflector continuity and better images geological features, such as faults and stratigraphic boundaries.

This attribute is useful in showing lateral extent of geobodies and it may have a good image of lateral extent of over pressured formation. Since amplitude information does not reliably shows over pressure effects, this attribute may have an advantage in showing the changes between over-pressure and normal pressure formation.

3.6 P-Impedance and Vp/Vs Ratio

This seismic attributes are the products of simultaneous amplitude offset (AVO) inversion of seismic data using density, P-wave velocity and Shear wave velocity components. The input to generate these attributes includes P-impedance, Vp/Vs and density computed from the well data to derive the low frequency band of the final inversion. All the partial stacks of the model are fed into a singular inversion workflow

resulting in a final inversion that accounts for phase changes, bandwidth, NMO and tuning effects of the seismic data.

Figure 23 Vp/Vs

Figure 24: P-Impedance

3.7 Relative Acoustic Impedance

Relative Acoustic Impedance is a running sum of regularly sampled amplitude values. Calculated by integrating the seismic trace, passing the result through a high-pass Butterworth filter, with a hard-coded cut-off at 10 Hz. The attribute shows apparent acoustic contrast, indicates sequence boundaries, unconformity surfaces and discontinuities. It can also indicate porosity or fluid content in the reservoir, which is helpful in the prediction of formations under high pressure.

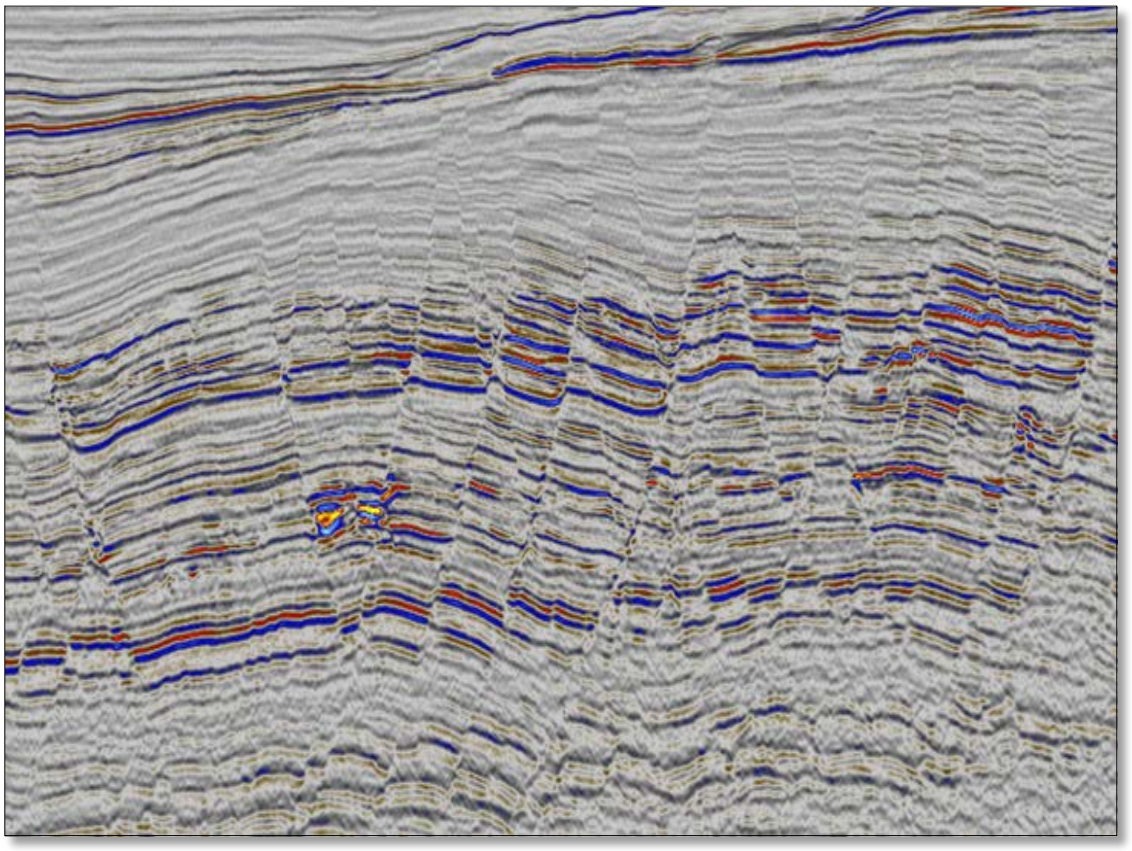

Figure 25: Relative Acoustic Impedance

CHAPTER 4

METHODOLOGY

4.0 Introduction

Most researchers have used the empirical relationship between seismic velocity and pore pressure to estimate pre-drill formation pore pressure. This method has yielded success in some limited local settings; however, often the results are masked by rock properties such as formation lithology and hydrocarbon content.

In this thesis, I present a novel method for digital pattern recognition called Support Vector Machine (SVM), to establish the relationship between 3D seismic attributes and actual formation pore pressure. The results of SVM and the selected training data (wells and seismic) are expected to yield results that isolate the pore-pressure-affected regime from other rock properties, such as lithology and hydrocarbon content.

4.1 Support Vector Machine (SVM)

SVM is a pattern recognition algorithm based on statistical learning theory that has been proposed by Vapnik (1998) and other researchers. This method performs classification of data using an N-dimensional hyperplane that best separates the data into two categories, it has a robust theoretical foundation which assures regularization and avoids over-training. Although SVM has a similar functional form to radial basis functions and neural networks, neither of these techniques incorporate the advanced theoretical approach to regularization that is the foundation of SVM.

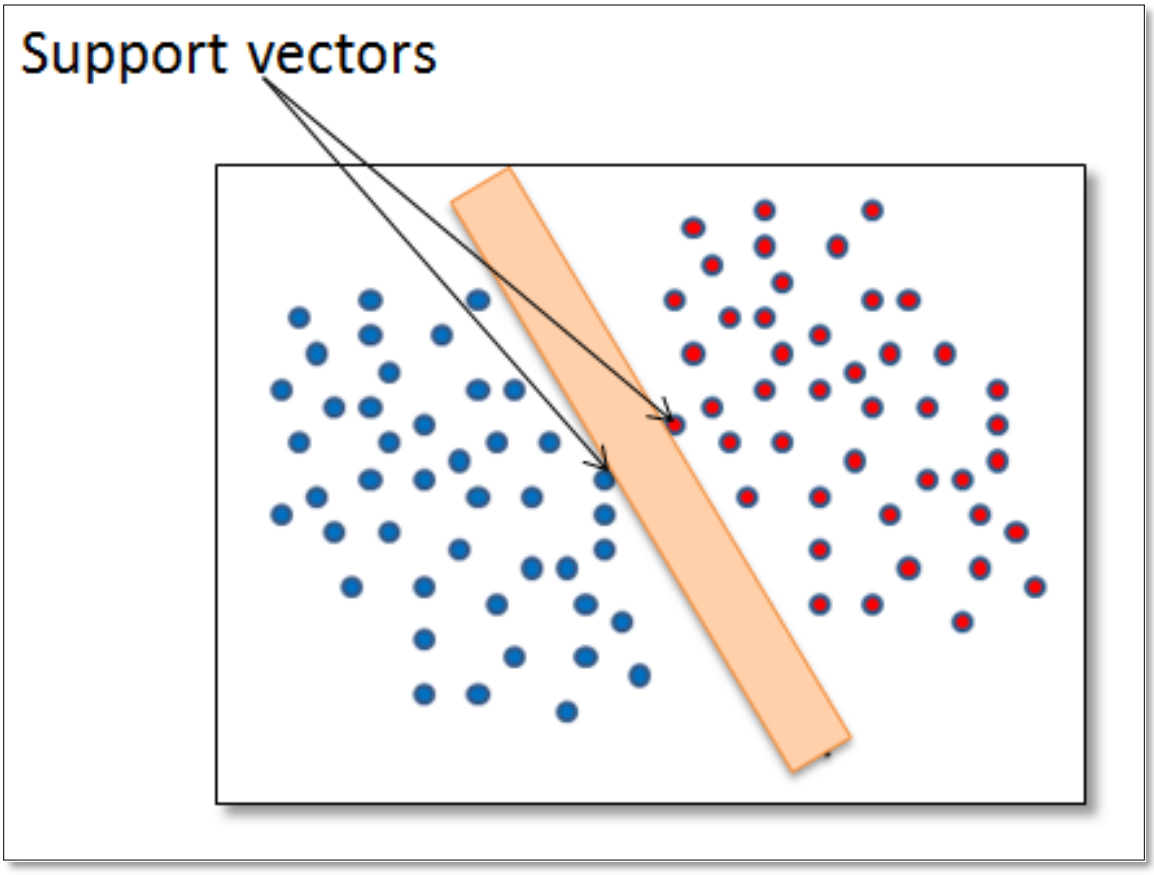

Figure 26: Simple, linear SVM example.

The generalization and ability to avoid overtraining, coupled with the ease of training of SVM improves its capabilities over traditional methods. In practical terms, SVM can model complex problems, such as text and image classification, bio-matrix, handwriting and speech recognition, and biosequencing. This novel algorithm is able to perform well on data sets that are composed of multiple attributes, regardless of how few actual training data sets are available. There is no constraint to the number of attributes that can be used in a given mode; which gives it a distinct advantage over traditional Neural Networks (Milenova et al, 2005).

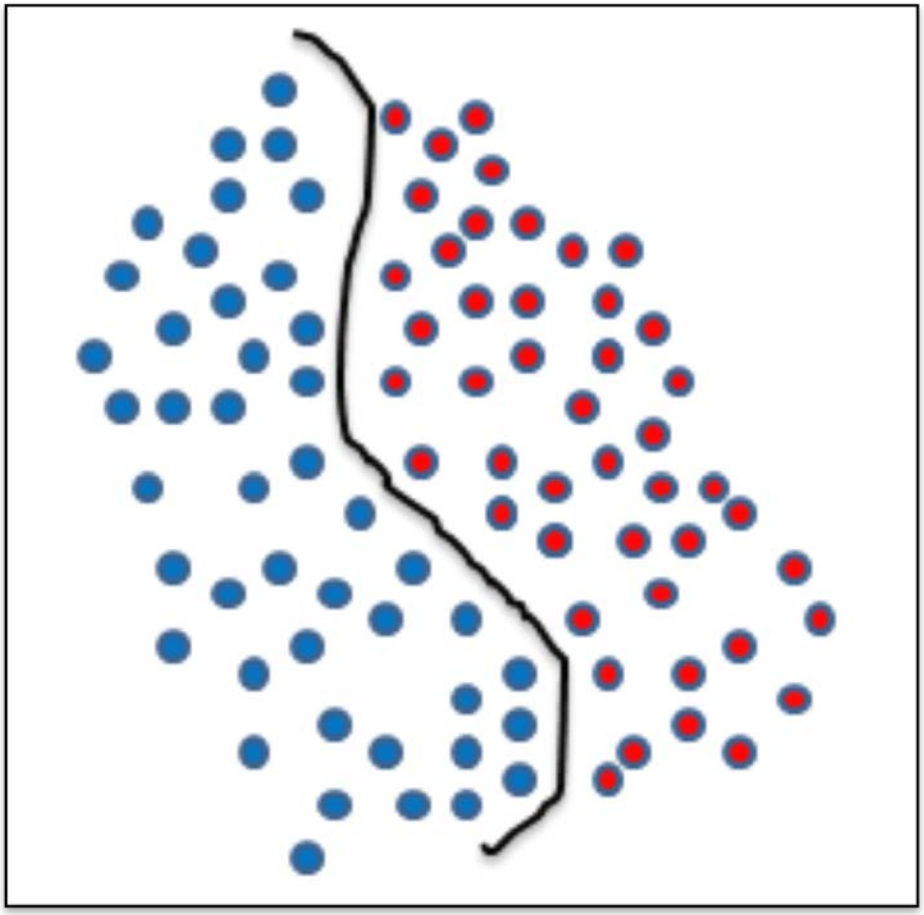

Figure 27: More complex linear SVM

An example of a simple linear Support Vector Machine is illustrated in Figure 26. In this example we have two data classes (Blue & Red) that are linearly separable. The separating line defines the border, on the right side of which is the Red data and the left side the Blue data. Any new object that falls on the right side is automatically classified Red and objects that fall on to the left side are classified as Blue (StatSoft, Inc.,2012).

This type of classifier is also called the Linear SVM and is characterized by the maximum margin of the line that separates the datasets. The data points that the maximum margin pushes against are called the "Support Vectors."

Most datasets are more complex than the example illustrated in Figure 26 and cannot be separated by a straight line. An example of a more complex scenario is illustrated in Figure 27. In this example, a complex structure is needed to separate the data classes; therefore, SVM utilizes a set of mathematical functions called kernels, to map the complex data into a higher dimension, where the data is linearly separable (see Figure 28). This mechanism of redistributing the data points is known as *transformation*. The resulting transformation of the data (based on learning data), avoids the need to construct a complex curve to separate the data (StatSoft, Inc., 2012).

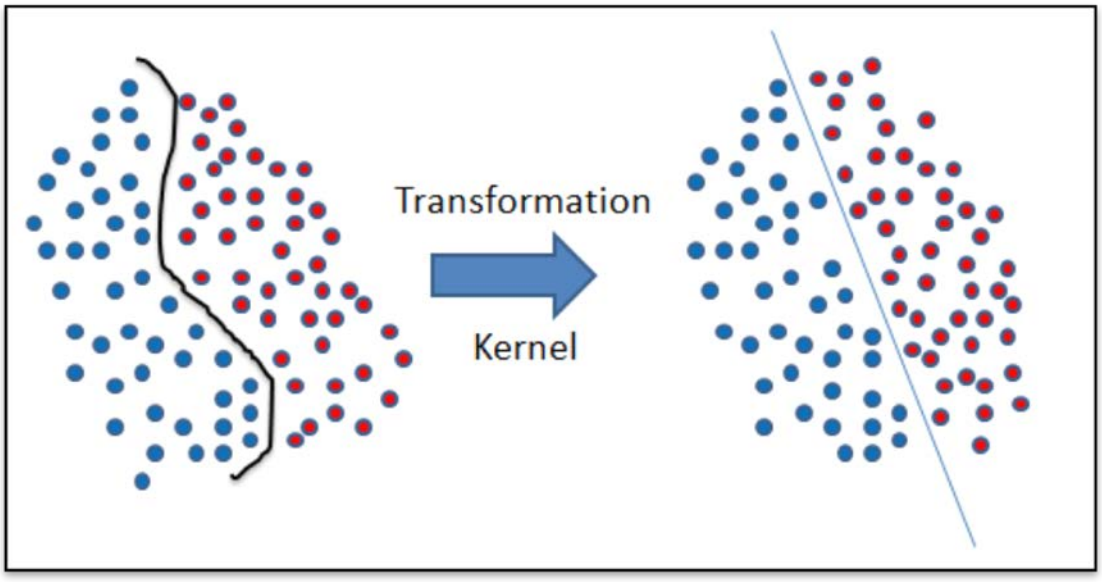

Figure 28: Complex classification transformation into linear classification via the SVM Kernel

There are several types of SVM implementations. In this Thesis, I utilize the regression SVM. An SVM function is represented by:

y = f(x) + noise

The task of this implementation of SVM is to find a function that can accurately predict new cases that the SVM has not been exposed to in the past. According to StatSoft, Inc.(2012), this task is accomplished by training the SVM model on a representative dataset (training data), which involves classification and the sequential optimization of an error function.

The algorithm will produce one dichotomy value if $\sum_{n=1}^{d}(w_i x_i) > Value$

And produce another dichotomy value if $\sum_{n=1}^{d}(w_i x_i) < Value$

Linear formulation of the hypothesis would look like $h(x) = sign((\sum_{n=1}^{d}(w_i x_i) - Value))$

In this implementation we use a Lagrange formulation to find the support vectors

$$\ell(\alpha) = \sum \alpha_n - \frac{1}{2}\sum\sum y_n y_m \alpha_n \alpha_m x_n' x_m - \sum \alpha_n$$

Maximize $\ell(\alpha) = \sum \alpha_n - \frac{1}{2}\sum\sum y_n y_m \alpha_n \alpha_m x_n' x_m - \sum \alpha_n$

The following matrix is then passed to the quadratic programming module:

$$Min(\alpha)\frac{1}{2}\alpha' \begin{matrix} y_1 y_1 x'_1 x_1 & y_1 y_2 x_1' x_2 & y_1 y_N x'_1 x_N \\ ..... & ..... & ..... \\ y_N y_n x'_N x_1 & y_N y_2 x'_N x_2 & y_N y_N x'_N x_N \end{matrix}$$

Dimentions of the matrix are NxN

The quadratic programing returns many α

Most of these will be zero and few will be none zero. The non-zero alphas are our support vectors.

CHAPTER 5

SUPPORT VECTOR MACHINE (SVM) IMPLEMENTATION

5.0 SVM Implementation

The implementation of SVM involves three steps:

1. Selecting training dataset. In this Thesis, the training dataset consists of well data and seismic attributes.
2. Implementing the SVM kernel to learn the pattern in the training dataset.
3. Implement the SVM to recognize the learned pattern in the whole seismic attribute 3D volume and generate a predicted target attribute volume.

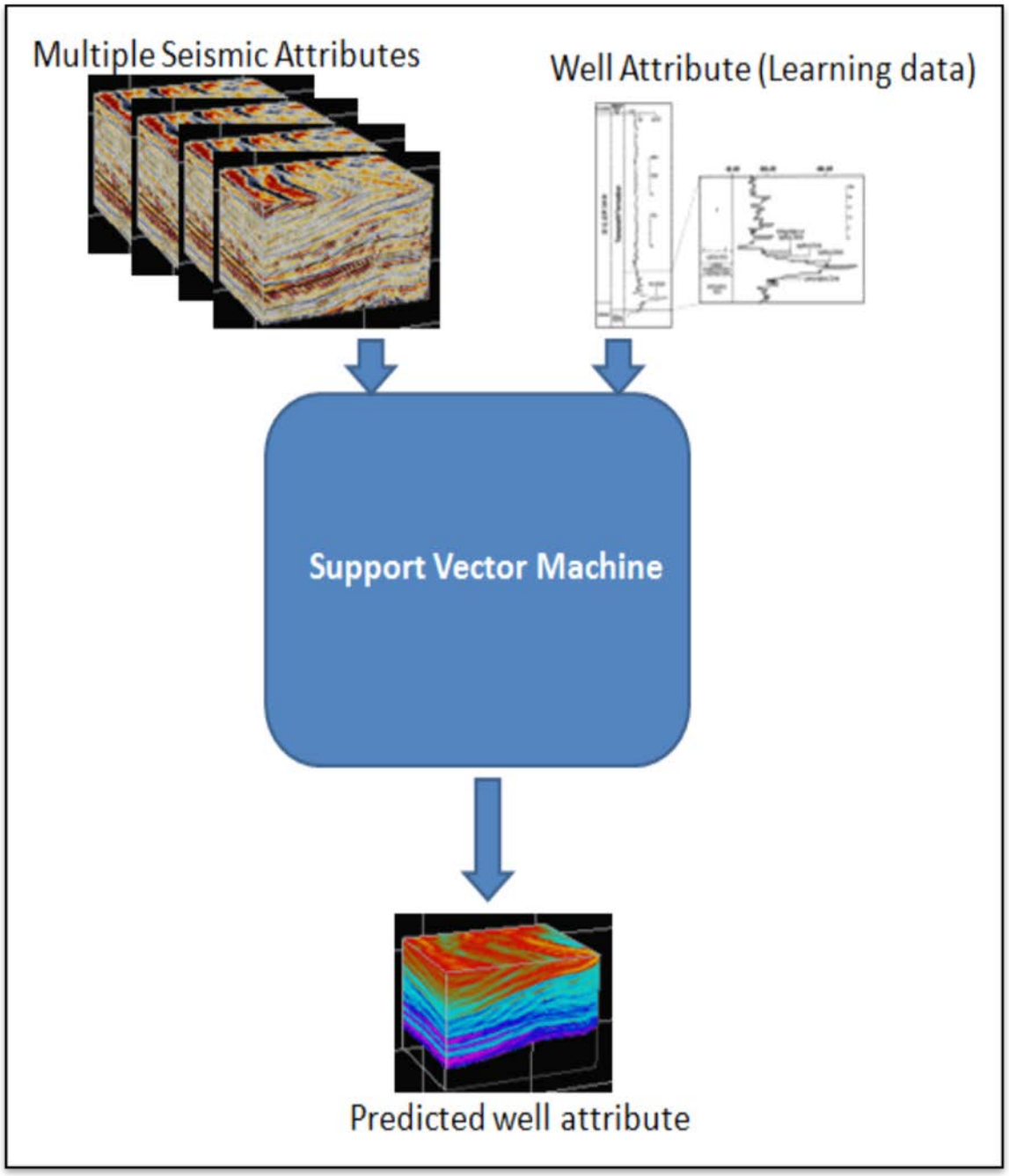

Figure 29: SVM Implementation workflow

5.1 SVM training seismic data

To guide the SVM algorithm I utilize the following eight seismic attributes:

1. Instantaneous Frequency
2. Average Frequency
3. Reflection Intensity
4. t*Attenuation
5. Cosine of Phase
6. Vs/Vp
7. P-Impedance
8. Reflective Acoustic Impedance

Before the SVM program is run, examination of all eight seismic attribute volumes alone showed no indication of where the high/low pore pressure areas of the section were located.

The eight seismic volumes were standardized to cover the same geographic area and prepared to be utilized by the SVM algorithm.

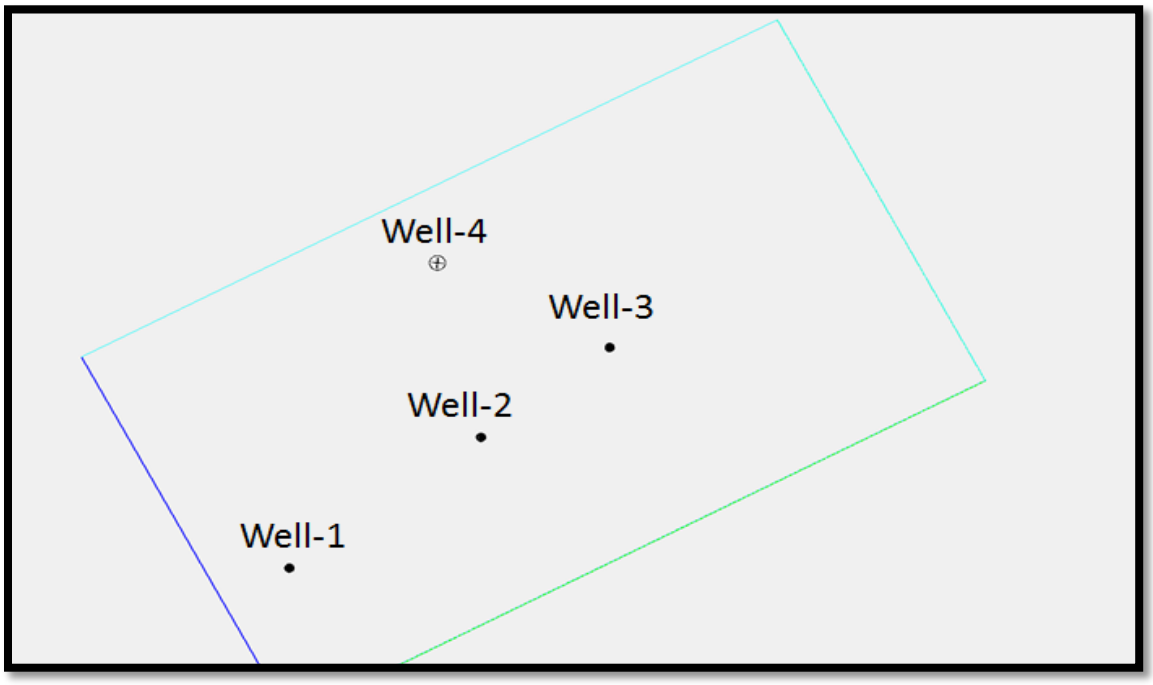

Figure 30: Map showing the relative location of the 3D survey, training wells (Wells-1, 2, & 3) and the blind test well Well-4.

5.2 SVM Training Well data

The Northwest Region of Saudi Arabia, particularly the Qusaiba formation, is characterized by higher than normal pore pressure. There are a number of wells drilled in the area and several of them have encountered over pressured rocks, making this a suitable dataset for this study. The study will utilize Well-1, Well-2 and Well-3 as the training dataset and use Well-4 as the blind test to validate the results of the SVM algorithm. The relative locations of these wells are shown in Figure 30 and 31.

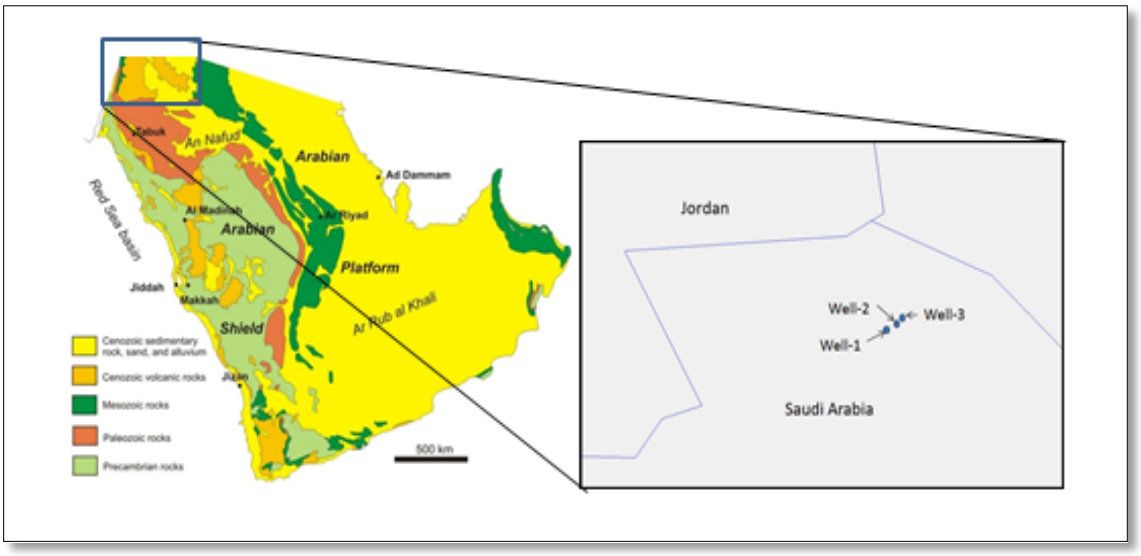

Figure 31: Location of training well data

5.3 Mud-Weight Log Curve

In this study, the mud-weight curve indicates the on-set of high pore pressure. A typical mud-weight curve showing changes in pore pressure is illustrated in Figure 32.

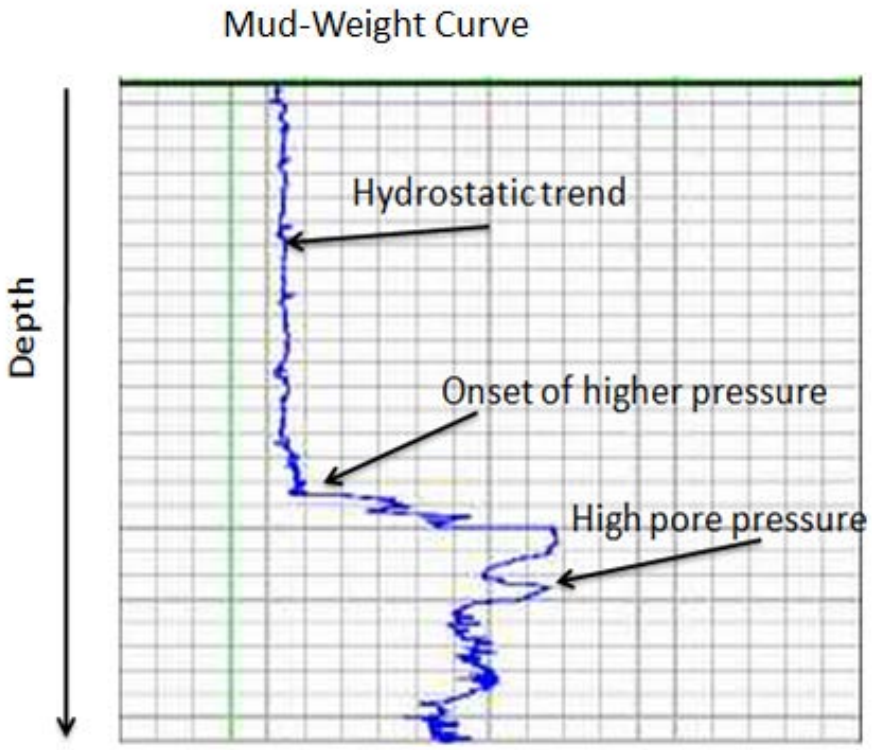

Figure 32: Example of Mud-weight log showing higher pressure trend

In drilling operations, the density of the drilling fluids (mud-weight) is used to balance the pore pressure to ensure safe drilling. Ordinarily, the mud-weight is kept slightly higher than the pore pressure to maintain well integrity, which causes slight invasion

of the mud into the formation. Since the mud is highly impermeable, its invasion into the formation is kept to a minimum, otherwise there may result formation damage that will lead to difficulties when testing or producing the well (Theys, 1991).

The rate of drilling progress (ROP) is also impacted by the mud-weight. Excessive mud-weight leads to slower ROP and results in inefficient drilling operations causing delays and premature wear of drilling equipment. Therefore, drilling engineers on a rig site are constantly adjusting the mud-weight to maintain a slightly overbalanced drilling pressure system.

While drilling a pressure transition zone, the pore fluids could suddenly increase due to the penetration of a pressure sealing formation. The slightly overbalanced mud system helps the drilling engineer to quickly react to this situation and maintain safe drilling operations. While drilling a pressure transition zone, the mud-weight is increased gradually ensuring well bore stability and maximizing safety.

The three wells used for training the SVM system all encountered pressure that was higher than the hydrostatic pressure during drilling of the Qalibah Formation. Drilling reports indicate gradual increase of pore pressure with a maximum pore pressure encountered on top of the base Qusaiba unit of the Qalibah formation. These reports also indicated a gradual increase of the mud-weight to counter the increased pore pressure. The plot of depth verses mud-weight curve shows the general profile of the pore pressure of the formations being drilled. There are a number of drilling-operation parameters that alert an engineer to the increasing pore fluids. The most apparent

indicator is the cut of the returning mud-weight due to influx of formation fluids or gas into the wellbore. When the mud-weight of the returning drilling fluids are lower than the injected mud-weight, then there is a presence of formation fluids that causes the reduction in the returning mud-weight. The drilling engineers typically react to this phenomenon by stopping the drilling operations, increasing the surface mud-weight and circulating the drilling fluids to seal the borehole and prevent the influx of formation fluids into the borehole. The drilling operations are resumed only when the returning mud-weight is equal to the injected mud-weight and a successful leak-off test is achieved, indicating no formation fluids are entering the borehole.

Another key indicator of higher pore pressure while drilling shale formations is the presence of shale cutting instability, characterized by the visibility of shale caving at the shale-shakers. The cuttings instability is produced by the reduction of in-situ stresses on the shale cuttings as soon as they are released from the formation and enter the borehole annulus. The uniform mud pressure, which may be lower than the formation pressure, allows the shale cuttings to swell and may provide enough forces to overcome the cementation strength and separate the clay platelets by drawing water from the mud system. Figure 33 shows a simplified schematic of the forces acting on a single set of clay platelets connected to a pore. Typical forces include the in-situ vertical and horizontal stresses, the pore pressure, the swelling pressure subjected to the clay platelets, and tensile or compressive cementation forces (Van Oort, 2003).

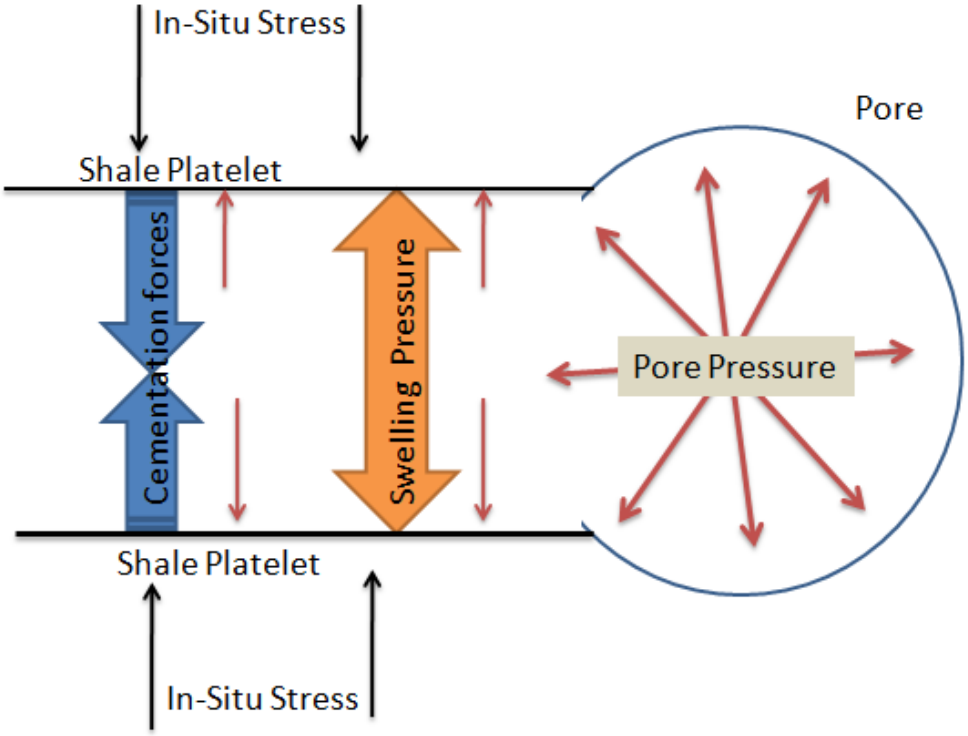

Figure 33: Simplistic schematic of forces acting on a set of clay platelets connected to a pore. Modified after Van Oort, 2003

5.4 Data Preparation for SVM

5.4.1 Well data

The current implementation of SVM for the prediction of formation pore pressure utilizes mud-weight curves to train the algorithm on areas of high pore pressure in the seismic data. As shown in Figure 32, the mud-weight curve is a good discriminator between formations under normal pressure and formations under high pore pressure.

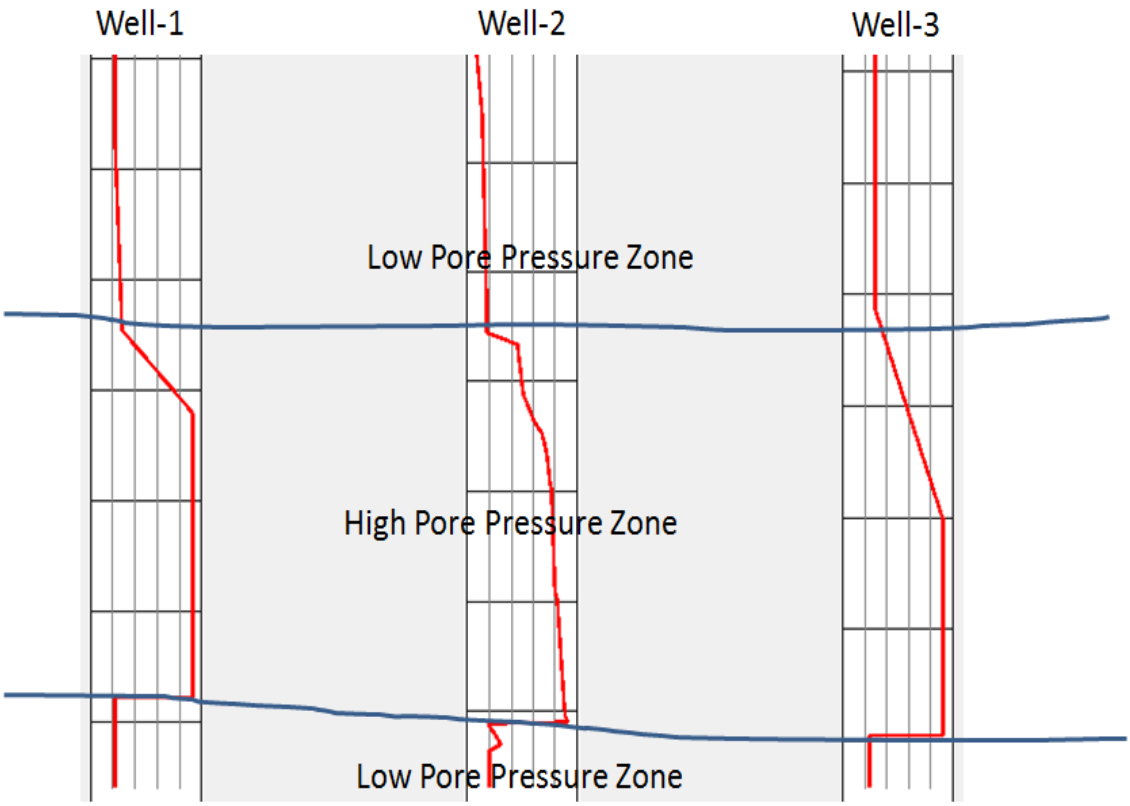

Figure 34: Mud-weight curve showing area of high/low pore pressure

During the investigation, I provided certain input data to the SVM program. This data was utilized as a learning data for the pattern recognition algorithm in SMV. The input data is described as follows:

1. Well description (wellsdscr.txt) file contains the surface location of the wells within the 3D survey area. The file also specifies the start time and increment of the mud-weight curve data in the wells.txt file. The format of the welldescr.txt file is shown in Table 1.

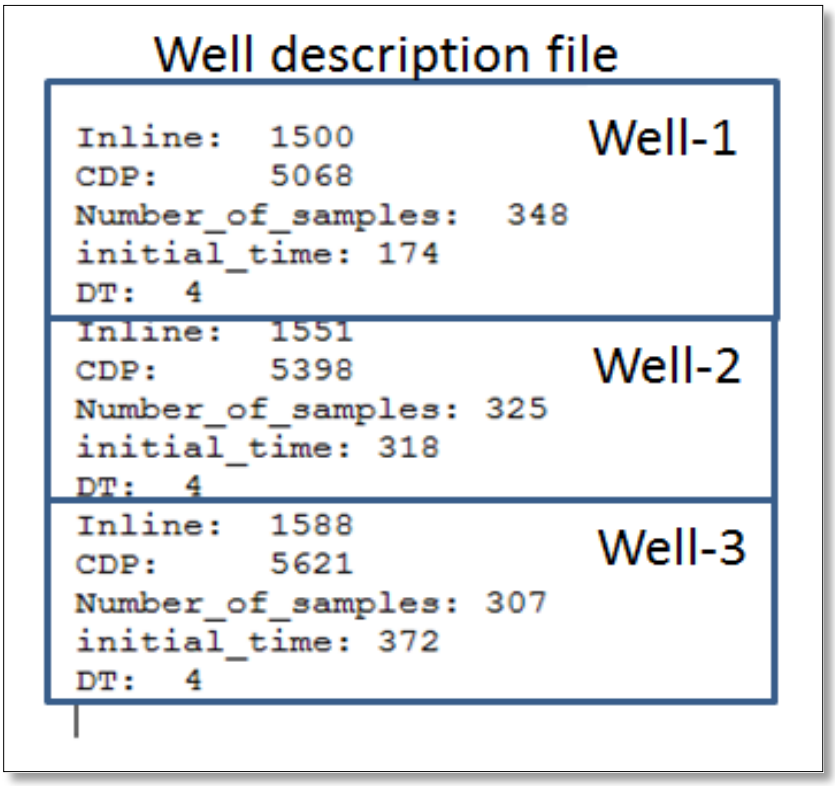

Table 1: Format of the welldescr.txt file (input to SVM)

2. The wells file (wells.txt) contains the list of well files that contain the mud-weight attribute data as specified in the wellsdescr.txt file above. Example well.txt is in illustrated in Table 2.

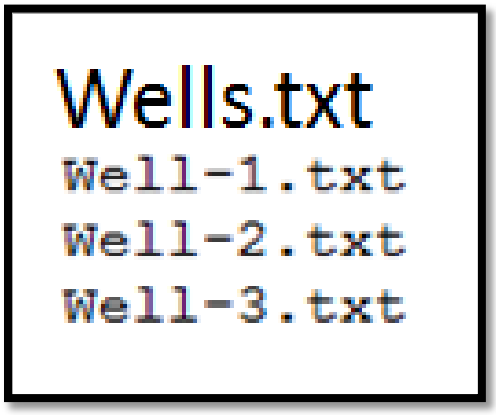

Table 2: Wells.txt file

3. For each of the training wells, there is a corresponding data file that contains the mud-eight values in a tabulated format. See example in Table 3.

Well-1.txt

72
72
72
82
82
82
83
83
83
84
84
90
90
91
91

Table 3: ASCII file showing Mud-Weight data for training well

4. The SVM program requires a parameter file to provide the values for certain parameters that are required. The format and structure of the parameter file (parameter.txt) is shown in Table 4.

```
nsubset: 0  #if 0, the size will be the number of wells
attribute_correlation_threshhold:  0 #if  ==0, all attributes will be used. it is within(0,1)
max_itr:  100      normally, keep it as is
show:  0           normally, keep it as is
eps:  1.0e-15      normally, keep it as is
fi_bound: 1.0e-15  normally, keep it as is
kernel_type:  RBF_kernel  normally, keep it as is
gamma1:    -5.0
dgamma: 1.0
gamma2: 15.0
c1: -5.0
dc: 1.0
c2: 30.0
traces_buffer: 5000
Segy_Inline: ffid
Segy_cdp:    cdp
output_file: pressure_volume_Jun20_2012.sgy
log_file:    pressure_volume_Jun20_2012.log
```

Table 4: SVM Parameter file content (parametr.txt)

The SVM program parameter file content is briefly described below:

Nsubset: The parameter controls the number of subsets — that the well data is divided into — to perform training and cross validation.

Attribute_correlation_threshhold: The threshold required to select/deselect the attributes. If the parameter is set at zero (0) all provided seismic attribute 3D cubes will be used and if it is set at one (1) none of the attribute cubes will be used. So, the range of this parameter is 0-1.

Gamma1: The parameter refers to the power item of the RBF kernel. For example, gamma1 of --5.0, will be translated to $2^{(-5)}$.

Traces_buffer: Number of seismic traces the program will hold in buffer during the prediction process.

Segy_Inline: ffid : Refers to the location of the inline in the SEGY trace header.

Segy_cdp: Refers to the location of the X-line in the SEGY trace header.

Output_file: Refers to the file name the output prediction volume will be written to.

Log_file: refers to the name of the log-file of the current run and will be time stamped.

5.4.2 Seismic Data

I generated eight seismic attribute volumes and utilized them as a training dataset for the SVM program to predict abnormal formation pore pressure. By themselves, none of these seismic attributes alone indicated abnormal pore pressure at the blind test location of Well-4. The significant impedance contrast between Qalibah shale formation and the underlying softer Sarah formation obscured any contrast in pore pressure between the two formations. The observed high pressure in the base Qusaiba in the training and blind test well was also obscured by the lithological change in the

interface between the Qusaiba and Sarah formations. Table 5 summarizes the correlation index of each seismic attribute volume and the mud-weight pressure indication curves at the well locations. Figures 35-41 show color displays of these input volumes at the bind test location of Well-4.

Seismic Attribute Volume	**Correlation Index**
Vp/Vs Impedance	0.431195
P-Impedance	0.291844
Attenuation	0.226091
Reflection Intensity	0.057949
Cosine of phase	0.041902
Reflection Acoustic Impedance	0.038487
Dominant Frequency	0.036325
Instantaneous Frequency	0.000906

Table 5: List of seismic attributes used for the pore pressure prediction and corresponding SVM index

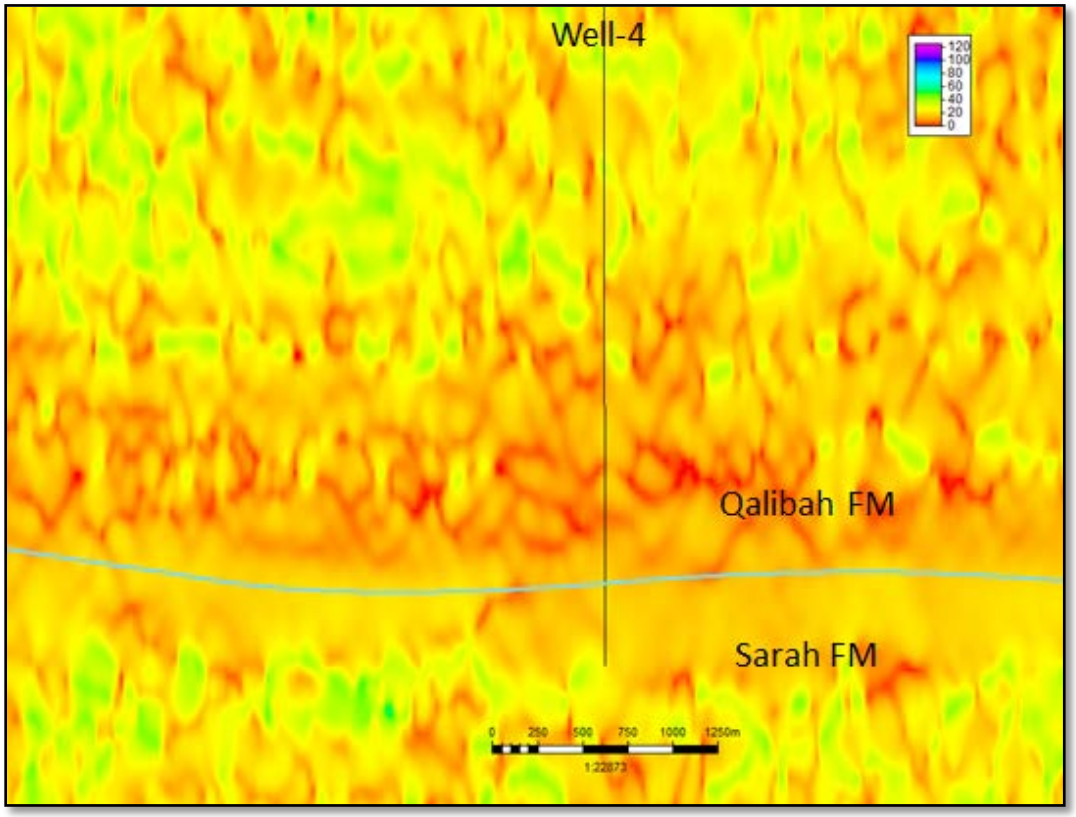

Figure 35: Instantaneous Frequency volume showing location of Well-4

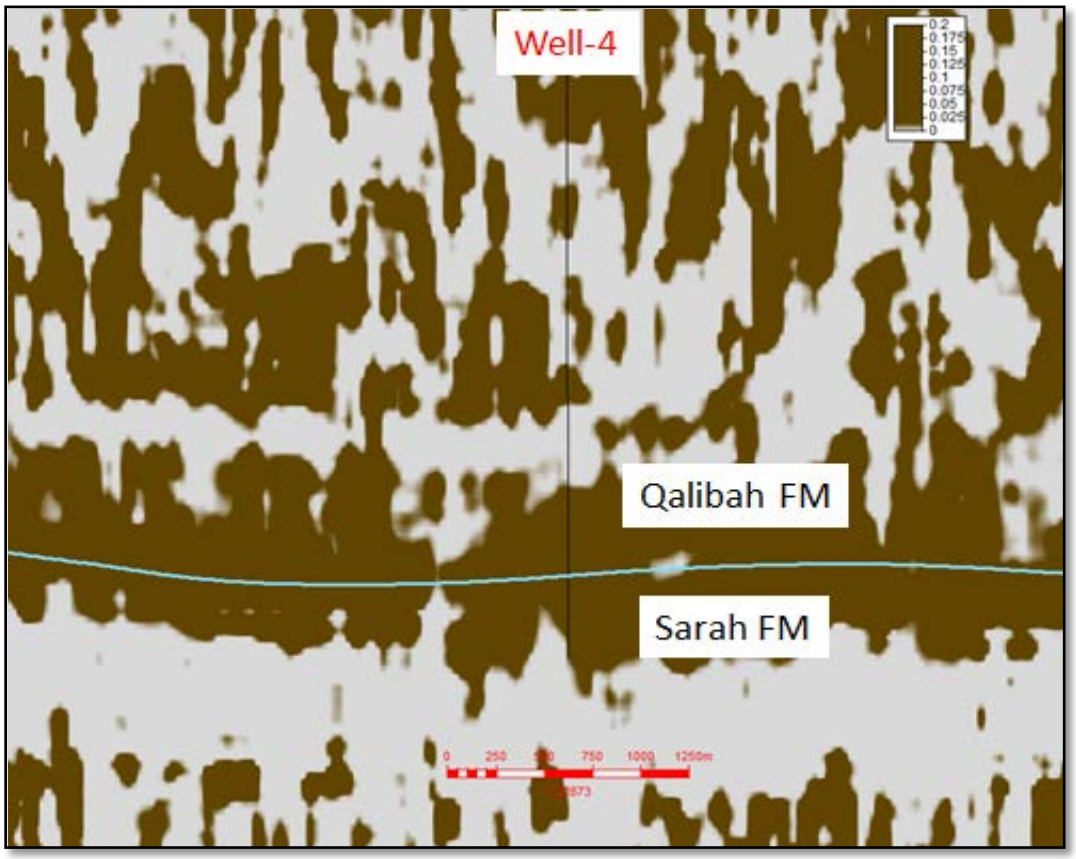

Figure 36: Attenuation volume at location Well-4

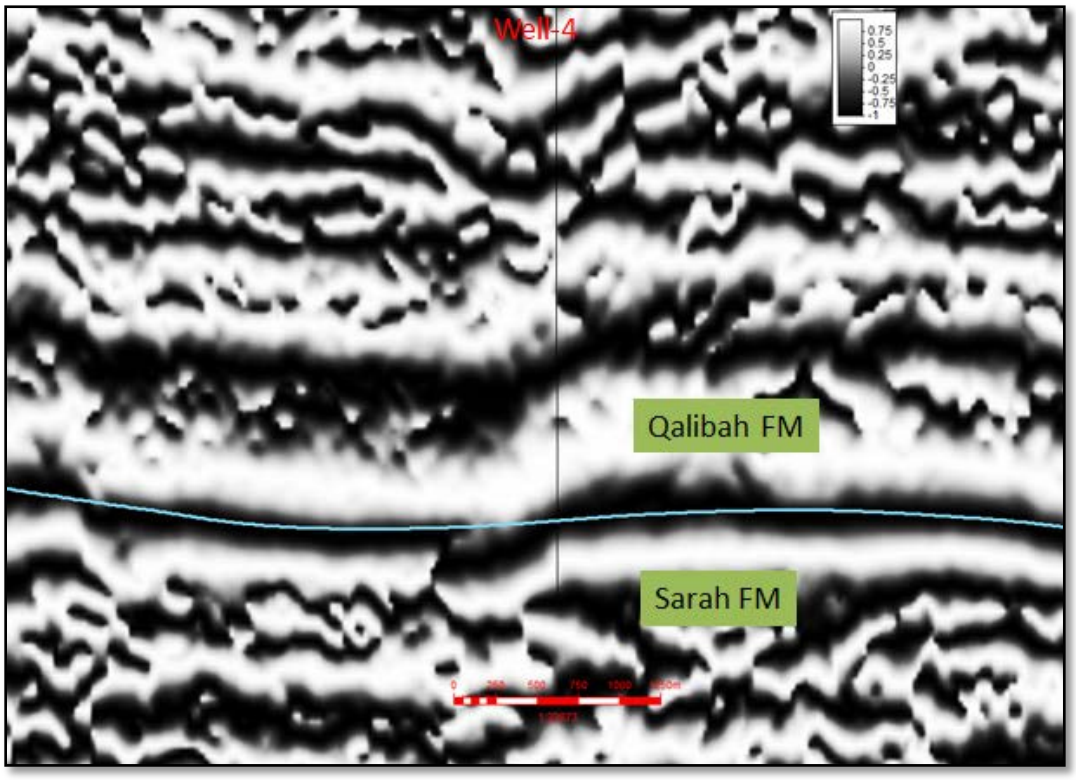

Figure 37: Cosine of Phase attributes volume

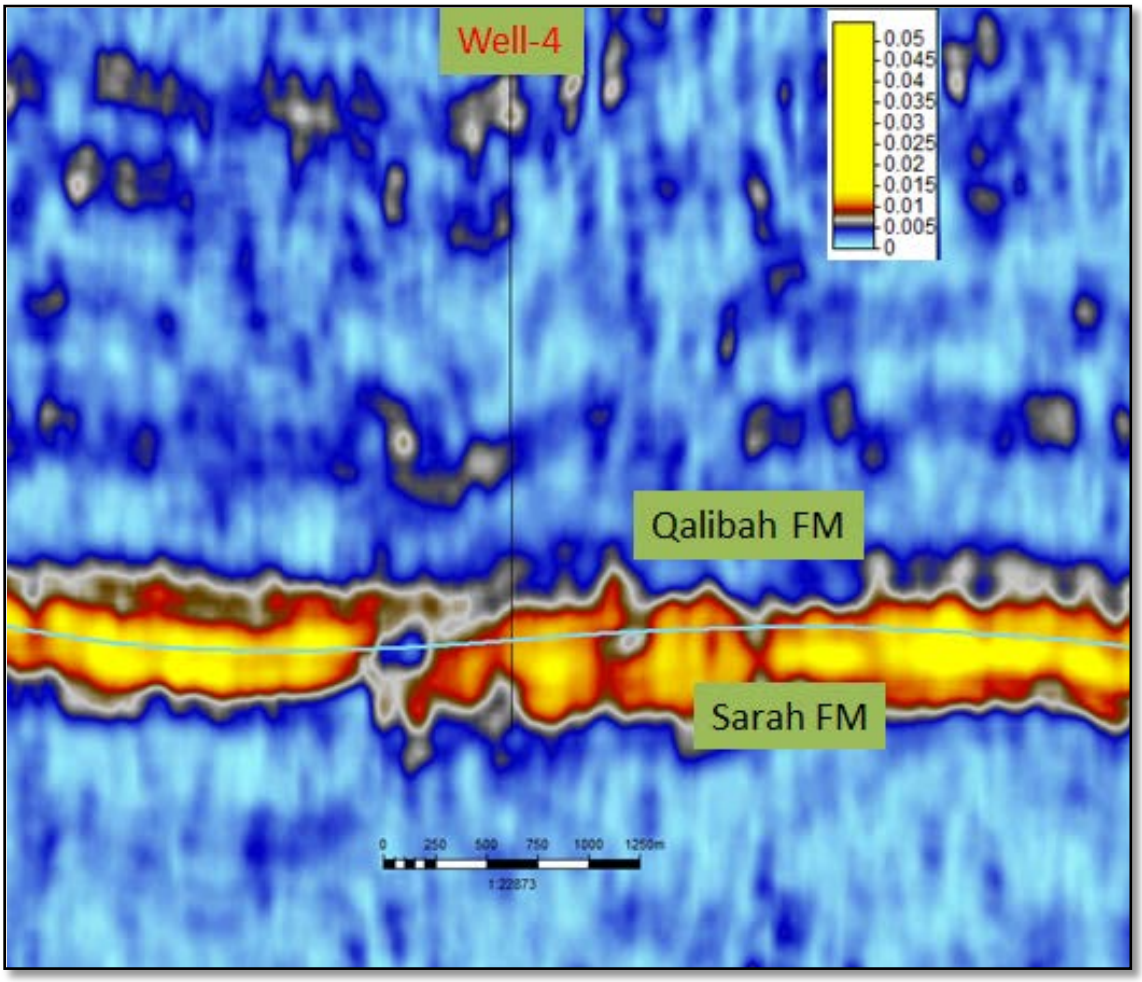

Figure 38: Reflection intensity seismic attribute volume

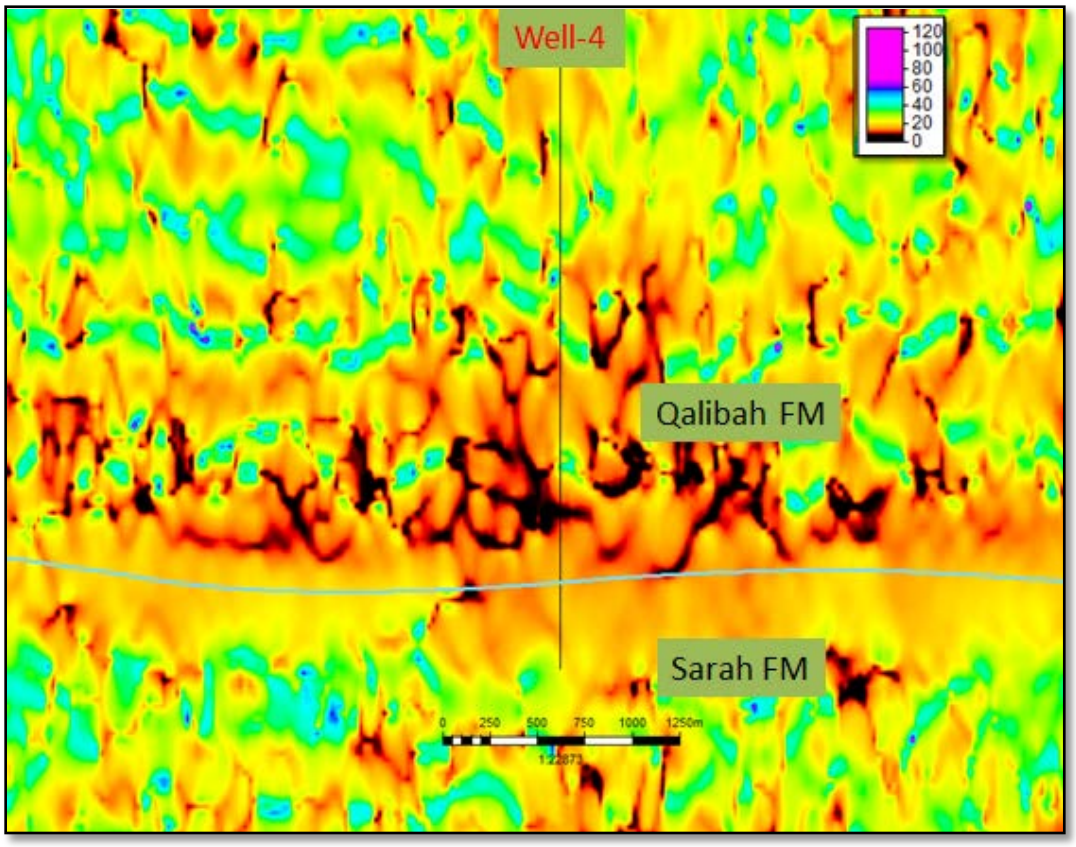

Figure 39: Dominant frequency seismic attribute volume

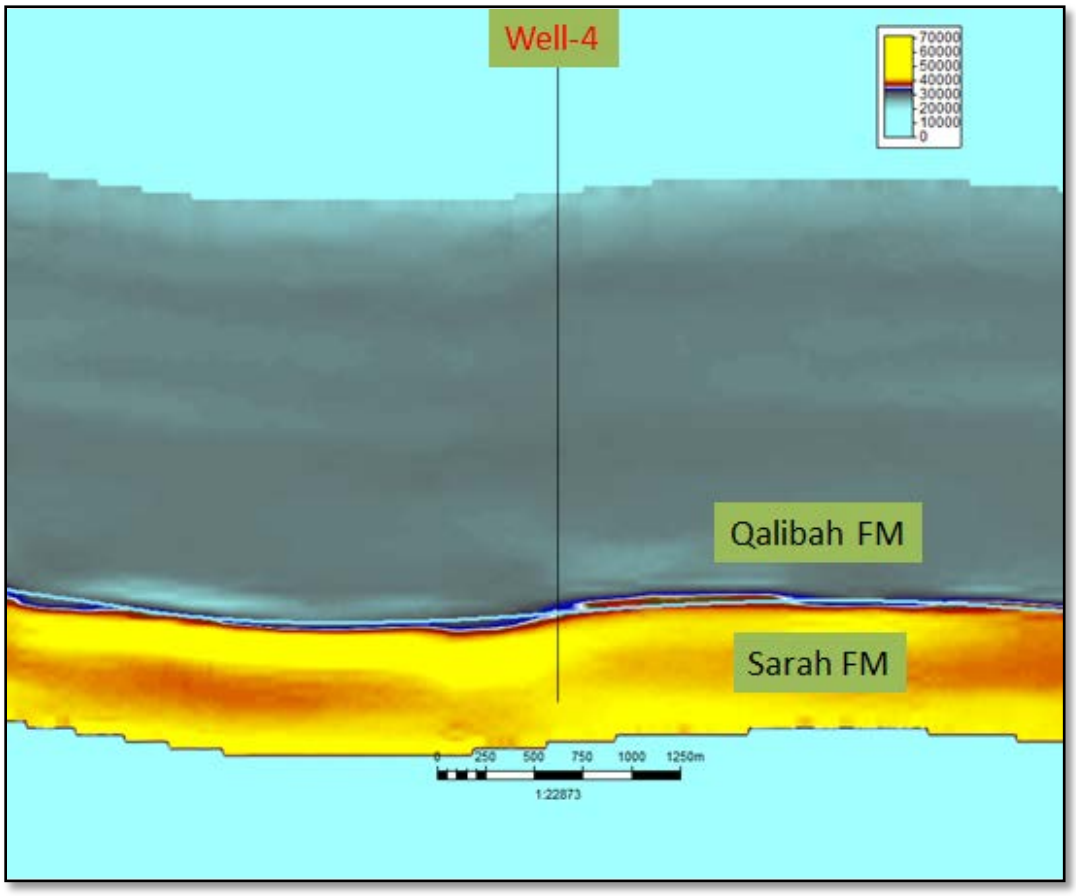

Figure 40: P-Impedance seismic attribute volume

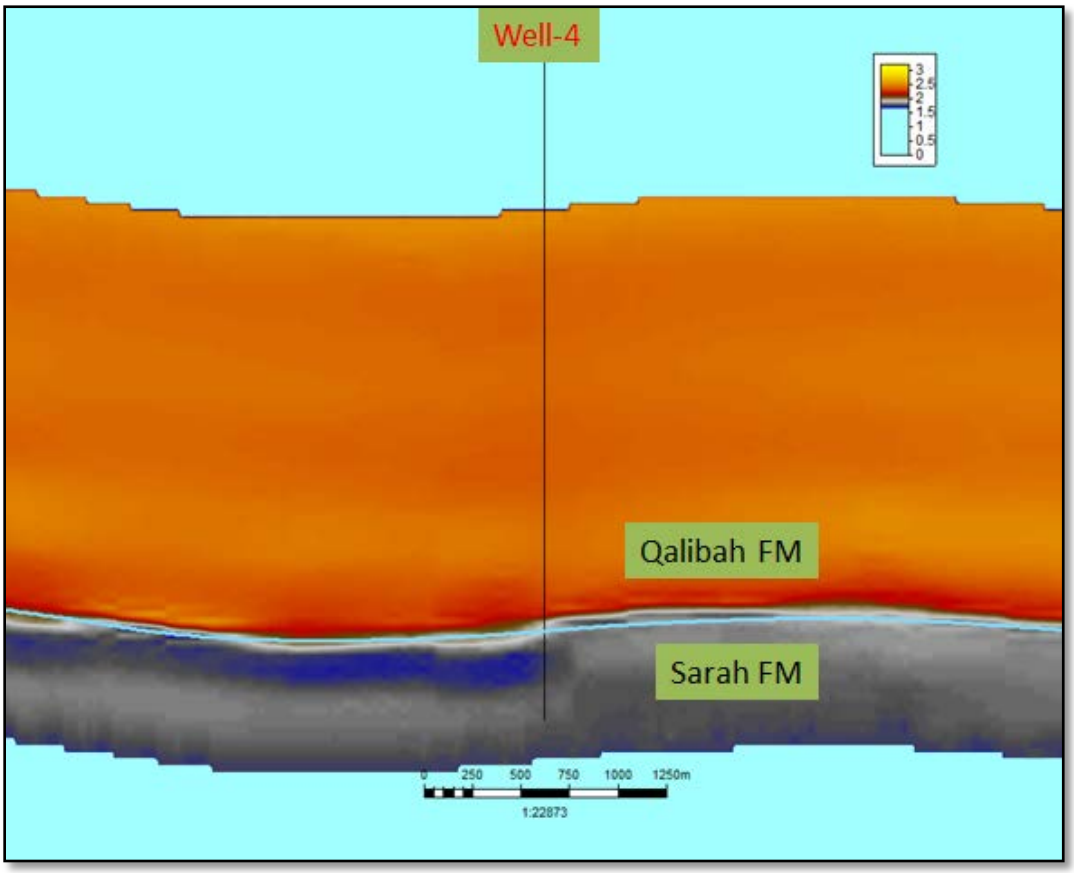

Figure 41: Vp/Vs-Impedance seismic attribute volume

5.5 Results of SVM Program to Predict Pore Pressure

The output from the SVM program is the result of the combination of all the seismic attributes and well data used as input. Based on the correlation index (Table 5), the Vs/Vp and P- impedance volumes had the most effect as they have a correlation factor of 0.43 and 0.29 respectively. These attributes are by far the most influential attributes of the results of the pore pressure prediction results. The data coverage of these volumes has been limited to an area centered on the base Qusaiba/Sarah formation boundary and so, the results of the SVM output relate to this range.

The blind test well (Well-4) was drilled approximately 7 km west of Wells1-3 that were used to train the SVM program. Well-4 encountered normal pore pressure condition on the top section of the Qaliba formation as have all the wells drilled in this structure. The drilling started to encounter abnormal pressure toward the bottom of the Qalibah formation. The mud-weight was raised to over 100 pounds per cubic feet (PCF) to counter the abnormally high pressure and control the well. The well also showed shale shavings and other high pressure indicators, such as rising formation gas and temperature, prompting engineers to raise the mud-weight to ensure safe drilling and proper well control.

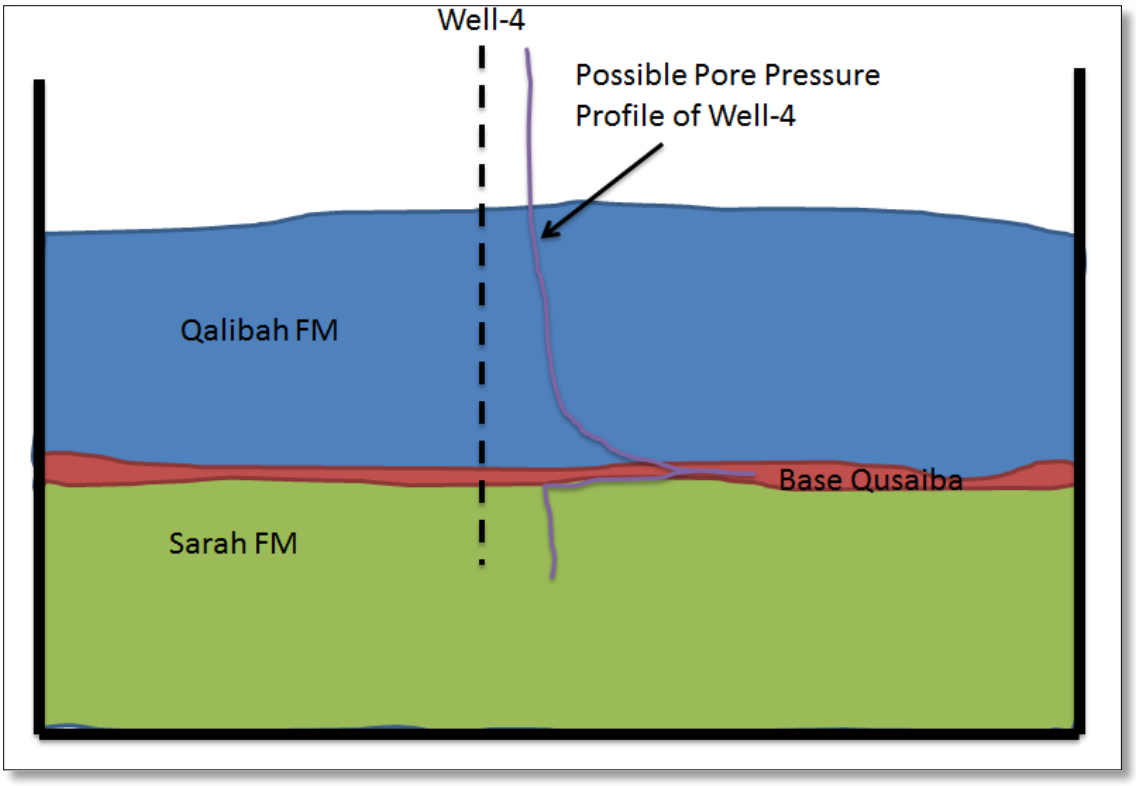

Figure 42: Schematic showing the pore pressure profile and the Qalibah/Sarah Formation.

Drilling of Well-4 was stopped at the base of the Qusaiba formation and casing liner set. The well was conditioned and normal pressure drilling mud-weight was utilized to drill the Sarah formation, which lies immediately below the base Qusaiba member of the Qalibah formation. This indicated that the two formations (Qalibah and Sarah) have different pore pressure regimes. The Qusaibah member exhibits high pore pressure and the Sarah formation shows lower pressure that is close to the hydrostatic pressure.

The SVM program shows very good correlation between the actual well attribute data (mud-weight) and the output mud-weight attribute seismic trace at the well location (see example on Figure 43).

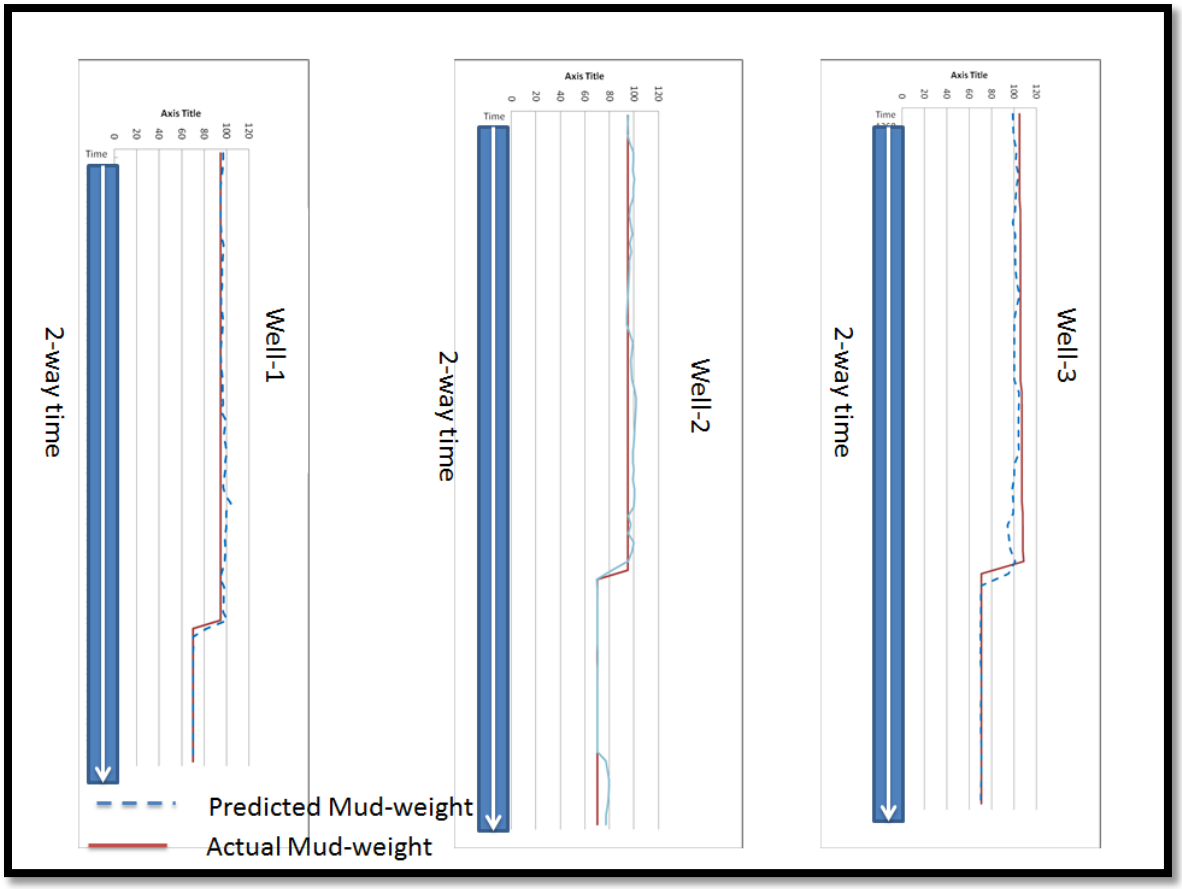

Figure 43: Comparison of actual well attribute mud-weight and the predicted mud-weight seismic attribute

The seismic attribute volume Inline at Well-4 shows remarkable details not found in any of the input seismic attribute volumes. As seen in Figure 43, the result of the SMV prediction shows a high degree of correlation with the actual well pore pressure conditions. The areas highlighted in red and yellow are areas where the well encountered higher pore pressure, and the areas in blue are those with lower pore pressure. The turquoise-blue section shows lower pressured Sarah Formation sections. This clearly shows the pressure contrast between the higher pressured Qalibah Formation and the hydrostatically pressured, underlying Sarah Formation.

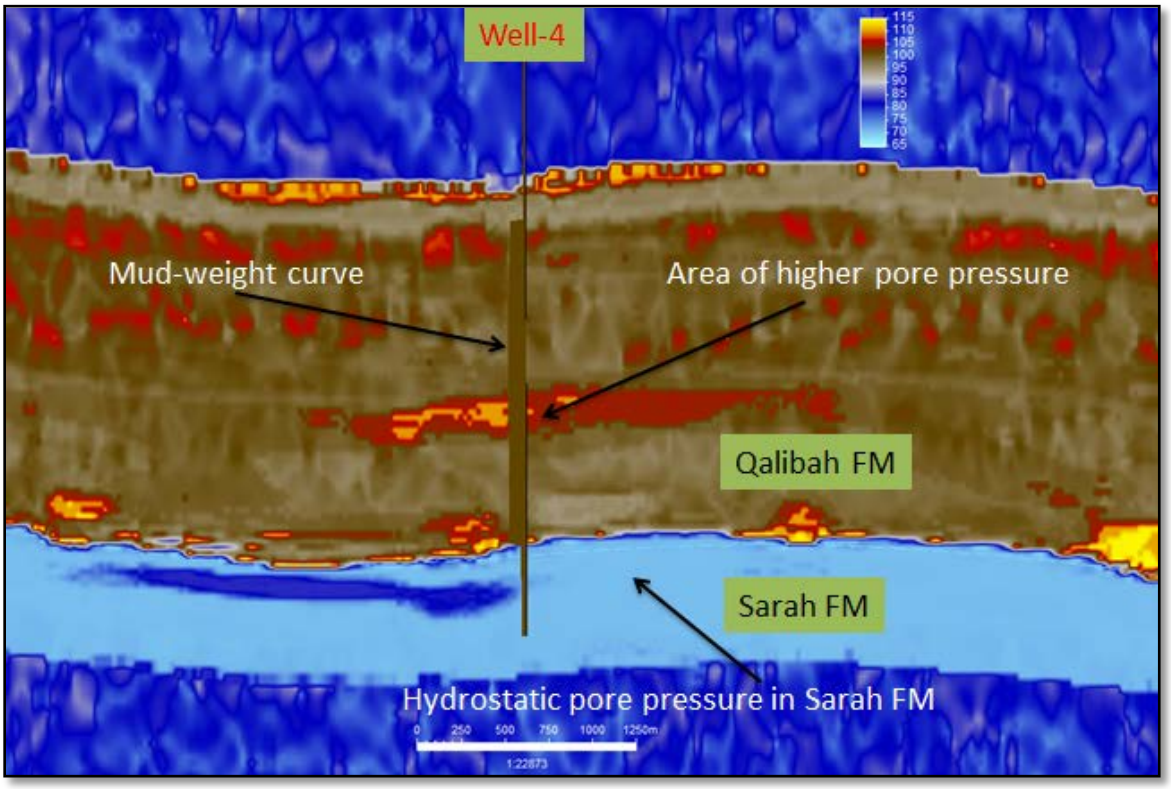

Figure 44: Inline section from the mud-weight seismic attribute volume intersecting the test well (Well-4)

The SMV results show not only the pressure variation in the Qalibah formation but also changes in the pressure regime of the Sarah formation. This could be significant for the targeting of fracture stimulation programs to produce hydrocarbons from sections of low permeability or porosity (tight sections).

From the mud-weight attribute volume, I extracted a trace at the blind test well (Well-4) borehole path and then constructed a predicted mud-weight profile of Well-4 (Fig 45). The predicted mud-weight curve at Well-4 can then be used to construct a predicted pore pressure profile of Well-4, using the following equation:

$$Pore\ Pressure\ (psi) = mud\ weight\ (ppg) * 0.052\ (psi) * 19.25$$

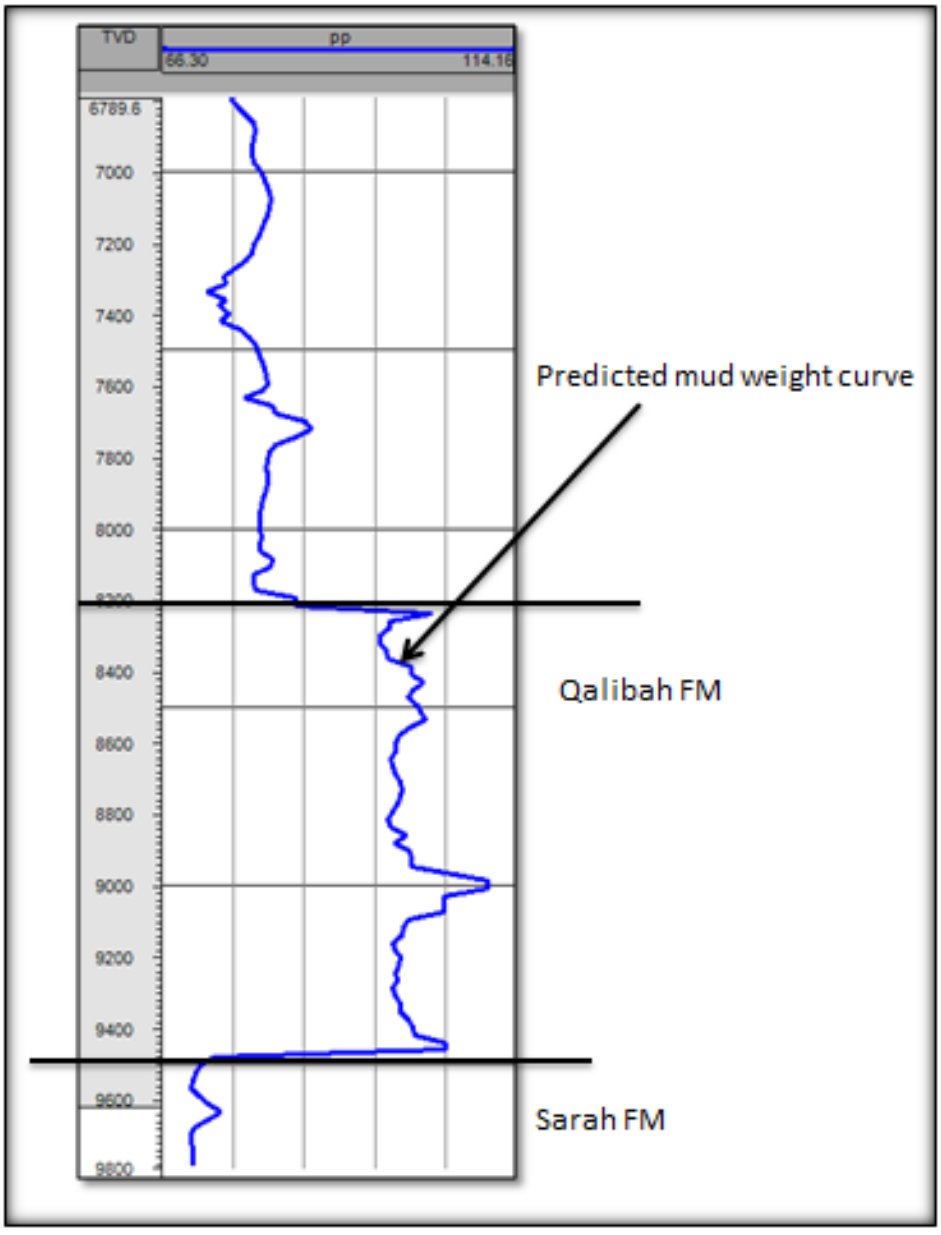

Figure 45: Extracted trace from the prediction mud weight volume

CHAPTER 6

CONCLUSIONS

6.0 Summary

Pore pressure prediction is crucial to the safety and successful development of hydrocarbon reserves. Since seismic data has a large areal extent, it makes sense to utilize this data to predict the pore pressure of a given field or a new prospect area. Researchers have utilized various methods to predict pre-drill pore pressure from seismic data. These techniques include seismic velocity models, seismic attributes, velocity seismic profiles and the like. The accuracy of the prediction always depends on local conditions, lithology, pore fluids, compaction, depositional environment and many other factors that influence the creation of abnormal pressure conditions.

Researchers have also shown that certain pore pressure prediction methods such as the empirical relationship between seismic velocity and pore fluid pressure are masked by lithology and pore-space hydrocarbon content. Therefore more robust and novel methods are required to better predict pre-drill pore pressure. One such method is the

application of pattern recognition algorithms — to learn the signature of over-pressure sediments on seismic data — and utilize that information to predict the pore pressure conditions away from the control points.

In this research project, I have chosen the SVM algorithm as the pattern recognition software that can learn and then predict the seismic signature of sediments under abnormal (above hydrostatic) pore pressure. SVM is based on statistical learning theory that estimates a function $A = (+1, -1)$, using as input training data from wells for which we know the pore-pressure trend, such that the function *A* accurately predicts new data points (x,y) that are generalized by the fundamental probability distribution *P(x,y)* of the pressure training data.

Most pore pressure datasets are complex and are not easily separable by a simple linear hyperplane without significant error. As a result, SVM has a built-in function to transform the complex dataset into a high dimensional feature space (hidden layer space) where linear hyperplane separation takes place. This capability allows to perform tasks in this larger dimensional feature space without actually performing explicit computations. SVM is also superior to other pattern recognition algorithms, such as Neural Networks as it avoids over-fitting of the data around the control points (Li et al, 2004).

I selected the northwestern area of Saudi Arabia as the focus of my research. In this area the Qalibah shale formation is the source rock for most of the hydrocarbons produced in the northwest and central Saudi Arabia. The “hot” Qusaiba shale member constitutes the bottom section of the Qalibah Formation and has been shown to contain abnormally high pore pressure in wells drilled in the area. Therefore, I used the mud-

weight from three wells drilled through the Qalibah formation for the training dataset. The mud-weight data have proved to be indicative of the pore pressure conditions of the target formations.

The other training dataset used includes eight seismic attributes (see Table 1) computed from a seismic survey covering the target area. The way of assembling the seismic attribute volumes and the well data and the various parameters of the SVM program are explained in detail in Chapter 4.

The result of the SVM program is a mud-weight seismic attribute volume that encompasses the whole structure of the drilled wells. A fourth well (Well-4), drilled in the same structure was used as a bind test of the predicted mud-weight attribute. The results were remarkable and showed very close correlation to the actual mud-weight that was used to drill this well. It is also very much apparent that by utilizing this method, drillers could minimize the potential issues related to unexpectedly drilling into abnormally high pressured formations.

The SVM program is fast and only requires a basic computer infrastructure that is available in most oil companies. The assembly of the data is what takes the most time, but it is faster than performing detailed seismic velocity modeling associated with traditional velocity based pore pressure prediction.

The results obtained in this research project can aid in avoiding the costly and hazardous task of drilling wells in high pore pressure environments such as in Northwestern Saudi Arabia.

6.1 Future Research

The predicting of pore pressure is difficult under most circumstances given the extent of uncertainties inherent in most geophysical measurements. One can achieve a level of accuracy by utilizing advanced scientific computer algorithms — such as SVM and other methods — that can determine a relationship between formation pore pressure and observed well data.

Future research could focus on the development of well data that continuously measure the pore pressure of formation.

The results I obtained in my research are indicative of borehole pressure; however, further research could be carried out to convert the predicted mud-weight volume to pore pressure volume. I was not able to find an empirical equation that would do the direct conversion of the mud-weight values to pore pressure to my satisfaction.

The current research advances the methods of pore pressure prediction and I sincerely hope that future scientists can continue the work started here and come up with ways to improve this procedure to predict pre-drill pore pressure even more accurately.

REFERENCES

Abed A, M, Amireh B, and Khalil B, 1993. Upper Ordovician glacial deposits in southern Jordan. *Episodes*, Vol. 16 Nos, 1&2. March and June 1993

Al Mustafa, H. and Saeed AlZahrani. 2001, Geopressure Detection Using Neural Classification of Seismic Attributes in Base Jilh Dolomite in Central Uthmaniyah, Saudi Arabia. *SEG Int'l Exposition and Annual Meeting*, San Antonio, Texas September 9-14, 2001.

Aoudeh, S. and Al-Hajri, S., 1994, Regional Distribution and Chronostratigraphy of the Qusaiba Member of the Qalibah Formation in the Nafud Basin, Northwestern Saudi Arabia. Middle East Petroleum Geosciences, *GEO'94*, Vol 1, April 25-27, 1994, Gulf PetroLink Manama, Bahrain

Bordenave M.L. 2002. Gas Prospective Areas in the Zagros Domain of Iran and in the Gulf Iranian Waters. *AAPG Annual Meeting* March 10-23, 2001, Houston, Texas

Bruce, B. and Bowers, G., 2002, Pore Pressure Terminology, *The leading Edge*, Vol. 21, No. 2, Society of Exploration Geophysicist.

Chopra S, Marfurt K. "Seismic Attributes for Prospect Identification and Reservoir Characterization". Geophysical Development No.11. 2007 Society of Exploration Geophysics Publication.

Dutta, N. C. "Deepwater Geohazard Prediction Using Prestack Inversion of Large Offset P-wave Data and Rock Model", *The Leading Edge*, V. 21, No. 2, February. 2002, pp. 193-198.

Doyen, P.M., A. Malinverno, R. Prioul, P. Hooyman & S. Noeth, L. den Boer & D. Psaila, C.M. Sayers, T.J.H. Smit, C. van Eden & R. Wervelman. 2004. "Seismic pore pressure prediction with uncertainty using a probabilistic mechanical earth model," *2004 CSEG National Convention*.

Eaton, B. A.: "The Equation for Geopressure Prediction from Well Logs", *SPE Paper #5544*, Annual Fall Meeting of SPE of AIME, Dallas, Texas, Sept. 28 – Oct. 1, 1975.

Ebrom, D., P. Heppard, M. Mueller, and L. Thomsen, 2003, Pore pressure prediction from S-wave, C-wave, and P-wave velocities: *73rd Annual International Meeting, SEG*, Expanded Abstracts, 1370–1373.

Faqira, M., Bhullar, A., Ahmed, A., "Silurian Qusaiba Shale Play: Distribution and Characteristics" *AAPG Search and Discovery Article #90122@2011*. AAPG Hedberg Conference, Austin Texas December 2010.

Fertl, W. H., 1976, abnormal formation pressure: *Elsevier Science Publ. Co., Inc. New York.*

Guo, X. He, S., Liu, K,, Song, G., Wang, X., and Shi, Z,. 2010, Oil generation as the dominant overpressure mechanism in the Cenozoic Dongying depression, Bohai Bay Basin, China. *AAPG Bulletin*, V.94, No. 12 (December 2010) PP. 189-1881

Ian Hillier, 2000, Origins of Abnormal Pressure, *Baker Hughes INTEQ internal publications*

Jaikang L., Castagna, J., Li, D., Bian, X. 2004. "Reservoir prediction via SVM pattern recognition," *SEG Int'l Exposition and 74th annual meeting*. Denver, Colorado, October 2004.

Konert, G.,A.M Afifi, S. A. Al-Hajri, K. de Groot, A.A. Al Naim, and H.J. Droste, 2001, Paleozoic stratigraphy and hydrocarbon habitat of the Arabian Plate, in M. W. Downey, J.C. Threet, and W.A. Morgan, eds, Petroleum provinces of the twenty-first century: *AAPG Memoir* 74, p. 483-515.

Kumar, K, Ferguson, R., Ebron, D., and Heppard, P. Pore pressure prediction using an Eaton's approach for PS-waves. *SEG Expanded Abstracts* 25, 1550 (2006); doi:10.1190/1.2369816

Le Heron, D., Craig, J., and Etienne, J. 2009, Ancient glaciations and hydrocarbon accumulation in North Africa and the Middle East. *Earth-Science Reviews* 93, P47-76.

Luning, S., Craig, J., Loydell, D., Storch, P., Fitches, B., 2000, Lower Silurian 'hot shales' in North African and Arabia: regional distribution and deposition model. *Earth-Science Reviews* 49, P 121-200

Mahmoud D., Vaslet D., Husseini M. 1992, The Lower Silurian Qalibah Formation of Saudi Arabia: An Important Hydrocarbon Source Rock. *AAPG Bulletin* V. 79 No 10 (October 1992), P. 1491-1506)

Mark Quakenbush, Bruce Shang and Chris Tuttle. Poisson impedance. *The Leading Edge*, February 2006.

Milenova, B.L., Yarmus, J.S., Campos, M.M., "SVM in Oracle Database 10g: Removing the Barriers to Widespread Adoption of Support Vector Machines," Proceedings of the 31st VLDB Conference, Trondheim, Norway, 2005.

McClure,H. A., 1978, Early Paleozoic glaciation in Arabia: Paleogeography, Paleoclimatology, Paleoecology, v. 25, p. 315–326.

Mujica, Daniel L, Aldajani, Abdulfattah. 2012. Pore Pressure Prediction from 3-D Seismic Data: A Feasibility Study of Unconventional Gas Exploration in Saudi Arabia. AAPG Search and Discovery Article #90141©2012, GEO-2012, 10th Middle East Geosciences Conference and Exhibition, 4-7 March 2012, Manama, Bahrain

Mukerji, T., Dutta, N., Prasad, M., and Dvorkin, J., 2002, Seismic Detection and Estimation of Overpressures: Part I: the Rock Physics basics. CSEG Recorder, September, 2002.

Mustafa, H. & Saeed Zahrani, S. Geopressure detection using neural classification of seismic attributes in Base Jilh Dolomite, in central Authmaniyah, Saudi Arabia. *Expanded Abstract presented at 2007 SEG Meeting.*

Schwehr, K., Tauxe, L., Driscoll, N., Lee, H. 2006, Detecting compaction disequilibrium with anisotropy of magnetic susceptilbity. Geochemistry, Geophysics, *Geosystems* (G^3) Volume 7, Number 11. November 3, 2006.

Spencer, J. W., 1981, Stress rexations at low frequencies in fluid-saturated rocks: Attenuation and modulus dispersion: J. Geophys. Res., 86,1803-1812.

Sarma L., Ravikumar N,2000. "Q-factor by spectral ratio technique for strata evaluation." *Engineering Geology* V. 57, Issue 1-2, June 2000, pp. 123-132.

StatSoft, Inc. 2012. Electronic Statistics Textbook. Tulsa, OK: StatSoft. Electronic version: http://www.statsoft.com/textbook/.

Sayers C., Woodward, M., and Bartman, R. Seismic pore-pressure prediction using reflection tomography and 4-C seismic data. The Leading Edge, February 2002, pp. 188-192

Taner M and Sheriff R. 1976"Application of Amplitude, Frequency and Other Attributes to Stratigraphic and Hydrocarbon Determination." *AAPG Bull*., v. 60, p. 528 -542.

Theys, P.P. 1991. Log Data Acquisition and Quality Control: Editions Technip.

USGS Fact Sheet FS-008-02,. U.S. Department of the Interior, U.S. Geological Survey. January 2002

Vaslet, D. 1990, Upper Ordovician glacial deposits in Saudi Arabia. Episodes, Vol 13. No. 3

Van Oort. E. Journal of Petroleum Science and Engineering 38 (2003) 213–235

Vapnik, V. 1998. Statistical Learning Theory. John Wiley and Sons, Inc., New York.

Vincent, P, 2008, Saudi Arabia: An Environmental Overview. Taylor & Francis

Young R.A and Lepley T, 2005. Five Things Your Pore Pressure Analyst Won't Tell You. *AADE 05-NTCE-12*.

Zhou S., Al-Hajhog, J., Simpson, M., Luo, M., Mohiuddin, M and Tan, C. 2009. Study of Jilh Formation Overpressure and its Prediction. *SPE/IADC Middle East Drilling Technology Conference & Exhibition*, 26-28 October 2009, Manama, Bahrain

CURRICULUM VITAE

- Abdoulshakour Ali Nour
- Born in Hargeys, Somalia in 1968. Moved to the United States of America in 1984.
- Graduated with a Bachelor of Science Degree in Geology from Oklahoma State University, in 1989.
- Worked as a well-site geologist for Exploration Logging (Exlog Inc.) a subsidiary of Baker Hughes Company (1990-1992).
- Jointed the Hunt Oil Company Gulf Coast Division in Houston, Texas USA as an Associate Geophysicist (1992-1996,).
- Worked for Pel-Tex Oil Company (1996-1999) as a Senior Geophysical Analyst.
- In 1999, Joined Saudi Aramco as an Exploration Systems Analyst.
- Received Masters of Science Degree in Geophysics from King Fahad University of Petroleum and Minerals, Dhahran, Saudi Arabia in April, 2013.
- Member of Society of Exploration Geophysicist, Dhahran Geological Society and Society of Petroleum Engineers.